CHAPTER 2

Methods for obtaining accurate access-tube TDR moisture in deep heterogeneous soils

[1]Benjamin F. Schwartz*, [1]Madeline E. Schreiber, [2]Penelope S. Pooler, [1]J. Donald Rimstidt
[1] Department of Geosciences
4044 Derring Hall
[2] Department of Statistics
Virginia Polytechnic and State University
Blacksburg, VA 24060
Phone: 1-540-231-7287 Fax: 1-540-231-3386
beschwar@vt.edu
*Corresponding author

Methods for obtaining accurate access-tube TDR moisture in deep heterogeneous soils

ABSTRACT

Hydrologic characterization of the vadose zone requires accurate measurements of soil moisture in a variety of soil textures. Time-domain reflectometry (TDR) instruments are commonly used to obtain soil moisture. Although there are advantages to using TDR, certain types of instruments pose challenges, including proper installation and calibration, which must be overcome. The principal objective of this study was to develop a new method for obtaining and calibrating access-tube TDR measurements in deep heterogeneous soils. Using two regression techniques, physical and chemical property-based calibrations were developed to predict soil moisture and explain unexpectedly large differences between TDR and field moisture values. Results provide insight into which physical and chemical parameters are most important for TDR calibration and lead us to propose new protocols for interpreting access-tube TDR moisture measurements. Differences between TDR moisture and gravimetric field moisture were almost entirely controlled by physical and chemical soil properties; indicating that our access-tube TDR probe likely produced an accurate measurement of 'free' but not the undetectable soil moisture. The undetectable fraction is controlled by physical and chemical properties and is a nearly static parameter at the depths and time scales considered in this study. Changes in TDR measurements after the initial calibration represent changes in the 'free' moisture content. Our calibration equations used easily obtained parameters to predict accurate soil moisture values in a wide range of soil textures. Approximately 95% of the soil moisture values predicted using our calibration equations had residuals of less than $\pm$ 10% soil moisture. We also developed a cost-effective method for installing access tubes which minimized problems related to air gaps and soil structure disturbances in deep soil profiles. This greatly increases the utility of TDR to be used as a tool for characterizing vadose zone hydrology in thick heterogeneous soils.

INTRODUCTION

Quantifying the spatial and temporal distribution of moisture in unsaturated porous media is critical to characterizing and modeling flow in the vadose zone. A variety of tools and methods have been developed to measure soil moisture in-situ. Because of its ability to acquire data quickly, and its relative safety when compared to nuclear methods (e.g., neutron probe), several different types of time domain reflectometry (TDR) probes are commonly used to measure soil moisture. Moisture measurements using TDR are derived by converting the measured bulk dielectric constant of a material, such as moist soil, into volumetric water content. Most TDR instruments are designed for long-term installation and continuous monitoring at shallow depths and are installed by inserting pronged wave-guides directly into the soil of interest, generally into the wall of a dug pit which is backfilled after installation. When deep vertical moisture profiling is required, this type of probe is not a practical option (Whalley et al., 2004). For these conditions, access-tube style TDR probes have been developed which allow moisture profiling using a single instrument that is raised and lowered inside an access-tube installed in the soil. Measurements are obtained without direct contact between the instrument and the soil of interest. Access-tube instruments can be used both for long-term installation and continuous monitoring of soil moisture or to obtain a single reading at a specific depth. From a hydrologic perspective, the main advantages of using an access-tube TDR probe include the ability to measure soil moisture profiles to greater depths and to obtain high spatial resolution using a single instrument.

Although TDR methods are useful in terms of their ease of use and ability to take measurements quickly, there are complications and challenges with using and installing TDR instruments. Modeling temporal variations in soil moisture profiles first requires the ability to accurately measure moisture in a variety of soil textures and over a range of depths. Thus, the most important question that must be asked when using TDR is: how accurate are the resulting soil moisture values? If TDR moisture values differ from gravimetrically obtained field moisture measurements, what are the reasons for this discrepancy? The only way to address these questions is through TDR calibration.

The traditional method for calibrating TDR measurements has been to use an empirical function which describes the relationship between moisture content and the bulk dielectric constant of a

soil (Topp et al., 1980). Alternatively, some researchers have calibrated TDR moisture measurements to soil moisture measured gravimetrically and/or with a neutron probe (Evett and Steiner, 1995; Laurent et al., 2005). With the TRIME probe used in this study, an initial calibration is applied to TDR measurements via an internally stored standard calibration equation that is assumed to be suitable for use in a wide range of mineral soils and will determine soil moisture values with a stated accuracy of $\pm$ 2 to 3% (IMKO, 2006a). It is also assumed that deviations from the standard equation are relatively small when measurements are made in different soil types: resulting in errors of only a few percent of soil moisture by volume.

For soils in which the standard calibration equations are not suitable, material-specific calibrations of TDR measurements to measured soil moisture values can be performed using one of several methods. For shallow soils, the most common material-specific method is to sample the soil of interest and develop a secondary empirical calibration equation in a laboratory setting by collecting multiple pairs of TDR moisture and volumetric moisture content measurements for individual soil samples (Chandler et al., 2004; Jacobsen and Schjonning, 1993). This method may be suitable for use in settings where a few samples from a relatively homogeneous field site will produce acceptable calibration results for soils in the area of interest. Unfortunately, the method is extremely time-consuming and is not practical for calibrating many individual TDR moisture measurements obtained in deep heterogeneous profiles. Additionally, for access-tube instruments, this method requires a very large soil sample which is very difficult to obtain in deep soils. A further limitation of this method is that it does not attempt to quantify the effects that various physical and chemical soil parameters have on the dielectric properties of a soil, and the resulting effects on TDR moisture measurements. As a result, it cannot be generally applied to estimate moisture in heterogeneous soils.

Another method for material specific calibration is to use a dielectric mixing model in which the modeled bulk dielectric constant is related to the individual dielectric values of specific components of the soil system including air, water, mineral grains and bound water (Dobson et al., 1985). By assuming a constant dielectric value for each parameter, a modeled value for soil moisture can be derived. However, in complex heterogeneous environments, variations in soil

texture, moisture content, mineral properties, and a variety of soil chemistry parameters make this type of model very difficult to apply.

A third method involves relating the bulk dielectric constant to soil moisture using volumetric water content, depth, and bulk density values determined from cores taken in a pit excavated adjacent to an access-tube (Whalley et al., 2004). In very heterogeneous conditions found at many field sites or in situations where significant depths are involved, this type of approach may not be practical either.

Although all the techniques discussed above have successfully been used to calibrate TDR measurements in relatively shallow soil environments, they are generally inappropriate or impractical for access-tube TDR measurements in deeper heterogeneous soils. Thus, after recognizing large differences between our TDR and field moisture values, the primary objective of this study was to develop a calibration protocol for access-tube TDR measurements based on statistical analyses of physical and chemical properties obtained from each of our soil samples. Our methods can not only be used to calibrate access-tube TDR measurements in similar settings but also to evaluate the relative influence of individually measured parameters (e.g., percent clay).

FIELD SITE

Our research site at the Virginia Tech Kentland Experimental Farms in Montgomery County, Virginia contains two well-developed sinkhole plains formed in ancient New River terraces (**Figure 2.1a**). Most sinkholes are broad and relatively shallow, allowing easy access for agricultural activities, and contain no bedrock outcrops. Thick terrace deposits mantle sinkholes with soils characterized as weathered fluvial terrace materials deposited by the ancient New River, which have developed over the underlying Cambrian aged Elbrook Formation limestone and dolostone bedrock. Soils are classified by the USDA-NRCS as Guernsey silt loam, Unison and Braddock soils, and Unison and Braddock cobbly soils (USDA-NRCS, 2006). Both sinkhole plains have numerous sinkholes of similar size and shape. Following initial characterization work of six sinkholes, two sinkholes were chosen for more detailed study. Sinkhole #1 is in a higher and older terrace deposit and contains highly weathered soils to depths

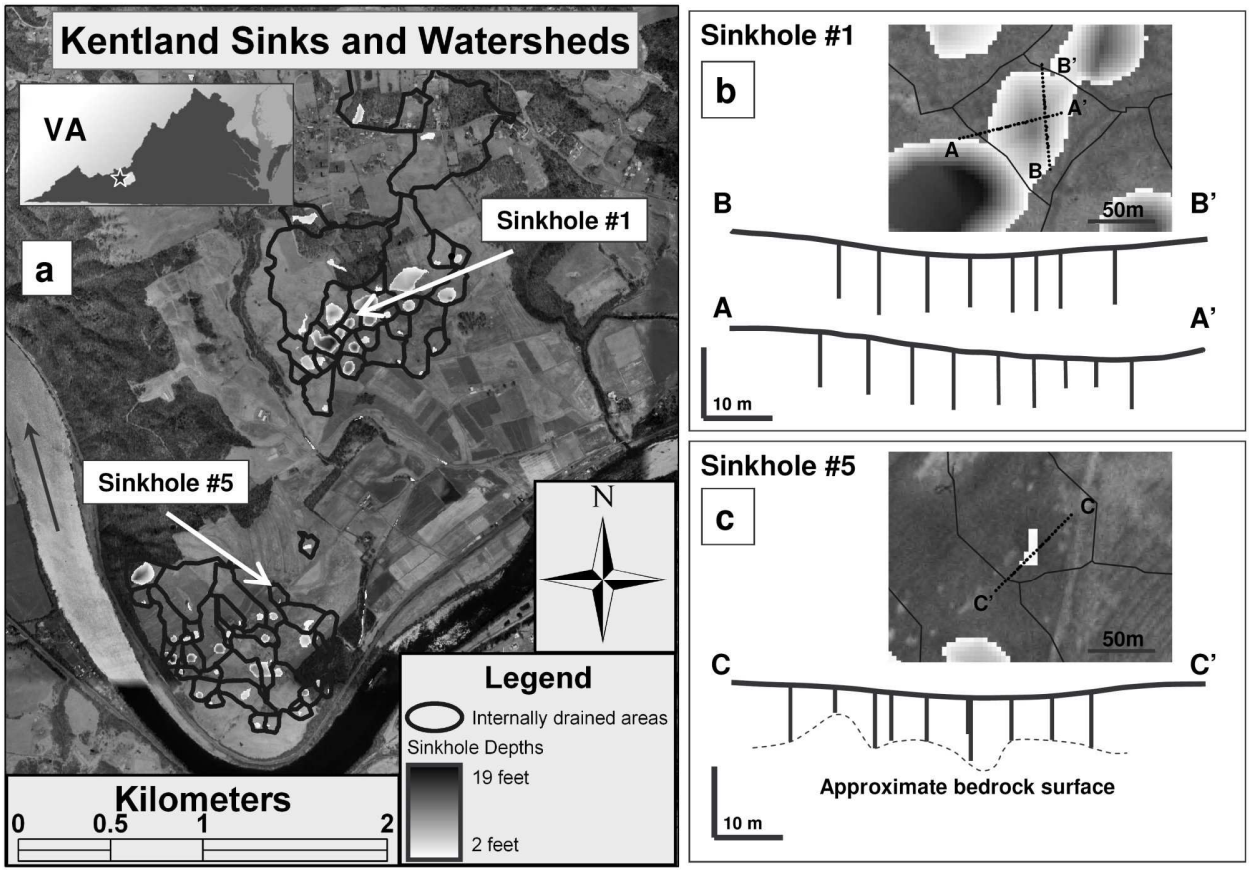

Figure 2.1 Study area and sinkhole transects

a) Virginia Tech Kentland Experimental Farms at Whitethorne, Virginia, USA. Figure 2.1a shows study sinkholes #1 and #5 and catchment areas (adjacent polygons) for each sinkhole within the two sinkhole plains. Aerial imagery © 2002 Commonwealth of Virginia. Sinkhole #1 is in the higher, older terrace. b) and c) show the location and orientation of instrumentation installed in transects across both sinkholes. Upper image in the diagrams is a map view of the sinkhole, while the lower portion of the diagrams shows profile views of monitoring wells, TDR access-tubes and other instrumentation installed along each transect. Note that depth of bedrock was not determined in Sinkhole #1.

of more than 40 feet (12.2 m). Sinkhole #5 is formed in a much lower and younger terrace and contains less weathered soils. In Sinkhole #5, bedrock was reached in nearly all augered holes at depths between 11 and 25 feet (3.4 and 7.6m) below land surface.

MATERIALS AND METHODS

Time Domain Reflectometry

At our field site, we used a TRIME T3-50 IPH Tube Access Probe TDR unit (manufactured by IMKO of Germany) connected to a laptop computer to measure and record uncalibrated percent moisture by volume. This instrument converts the pseudo-transit-time (which is related to the bulk dielectric constant) of a high frequency electromagnetic pulse into an approximate TDR moisture value using a factory-set internal calibration. Our instrument's internal calibration relates pseudo-transit-time to soil moisture using a standard equation in the form of (1). θ_{TDR} = TDR soil moisture [%] and t_p = pseudo transit-time.

$$\theta_{TDR} = -50.18321 + 0.769028 t_p - 4.19107 \cdot 10^{-3} t_p^2 + 1.185743 \cdot 10^{-5} t_p^3 - 1.613228 \cdot 10^{-8} t_p^4 + 8.57611 \cdot 10^{-12} t_p^5 \qquad (1)$$

Equation (1) is used by IMKO to initially calibrate each TRIME T3-50 IPH probe. After the initial calibration is performed, an instrument-specific calibration is then applied. Separate material specific calibrations can later be applied by the user. However, the instrument does not allow bulk dielectric constant values or pseudo-transit-times to be measured or recorded directly, and the final internal calibration coefficients are not accessible by the user. The T3-50 IPH probe has a stated maximum region of influence of 2.4 inches (60 mm) radially along the short axis of an oval field, and 6.3 inches (160 mm) on the long axis (MESA-Systems, 2006). Although multiple measurements at different angular orientations can be averaged to obtain a better estimate of soil moisture at a given depth, only one oriented reading was taken each time TDR moisture measurements were collected, as field experiments at our site showed little variation resulting from changes in angular orientation. Vertically, the T3-50 IPH probe measures the average moisture content over a depth interval of approximately 6 inches (15.24 cm).

Access-tube installation

TDR measurements for this study were collected from access-tubes installed in three transects across the two sinkholes between June, 2005 and May, 2006. Transects cross the low point of each sinkhole and radiate outwards to the edges (**Figure 2.1b** and **c**). Locations were chosen based on results of previous electrical resistivity tomography (ERT) surveys which indicated linear features such as 'valleys' in subsurface soil properties. The TDR transects follow and cross these features which, when more completely understood, will aid in future hydrologic characterization and modeling efforts at the site.

Transects consist of 15 access-tubes for two transects in sinkhole #1 and 8 access-tubes for the remaining transect in sinkhole #5. To install the access-tubes, a 2-inch (5.08 cm) mud-auger, custom manufactured to bore a 2.375-inch (6.03 cm) diameter hole, was used with threaded extensions to hand auger twenty-three holes to depths between 12 and 30 feet (3.6 and 9.1 meters). Schedule 40, 2.375-inch (6.03 cm) outer diameter PVC access-tubes were installed in the vertically augered holes. Access-tubes consist of standard threaded and o-ring sealed-joint PVC well-casing sealed on the bottom with a glued PVC well-point to seal the bottom. Care was taken to minimize air gaps between access-tubes and the surrounding soil. This is critical for obtaining accurate TDR readings because the dielectric constant of air is significantly lower than that of damp soils. Relatively small air gaps can thus produce significant errors in TDR measurements. During installation, access-tubes fit very snugly in augered holes to depths of 3 to 5 feet (0.9 to 1.5m). Below this, the fit was tight enough to require significant steady force to install, with resistance caused primarily by increasing friction between the tube and damp clay-rich soils, and compressed air in the augered hole beneath the sealed bottom of the access-tube. As a result of the tight fit and minimal vibration during installation, air gaps and soil disturbances around our access-tubes are assumed to be minimal.

The depth of individual holes was limited by cobbles or bedrock encountered and/or practical limits of hand-augering and sampling in deeper holes. To pass obstructing cobbles, we constructed a rock-breaking tool that could be threaded onto the auger stem to break smaller cobbles and permit a deeper hole to be augered.

After installation, access-tubes were completed by digging a shallow hole around the top of the tube and cutting the access-tube off just below ground surface. A removable end-cap was then used to seal the top of the tube. A protective cover consisting of a 12-inch (30.5 cm) length of 4-inch (10.2 cm) diameter Schedule 40 PVC pipe with an end-cap was then driven into the ground around the upper portion of the access-tube until the end-cap was flush with the ground surface (**Figure 2.2**). This was necessary to protect the access-tube from farming activities at the field-site. We recognize that this will influence long-term moisture measurements in the uppermost portion of the moisture profile.

Soil sampling

During augering for access-tube installation, volumetric soil samples were collected at one-foot (30 cm) intervals in most holes, with some holes having a two-foot (61 cm) sample interval. Sample lengths were taken by carefully measuring the depth of the auger stem before and after filling the auger, and not by measuring the length of the augered soil sample itself. Sample lengths averaged 5.0 inches (12.7 cm) and were recorded for use in volume calculations. Sample volume was calculated by multiplying the augered depth of each sample by the augered cross-sectional area (28.6 cm^2). To preserve original field moisture content, each soil sample was removed from the auger and placed in a labeled zippered polyethylene bag for later lab analysis. A field-log recording depth and thickness of each soil horizon encountered included details on soil color, difficulty in augering, approximate soil texture, relative moisture content, and amount and type of gravel or cobbles observed. After installing each access-tube, TDR moisture measurements were immediately recorded at 6-inch (15.2 cm) depth intervals in the access-tube.

Sample analysis

Each sample was weighed to the nearest 0.01 g prior to drying in an oven at 105°C until repeated weighing showed no further weight loss. A final oven-dry weight was then recorded. Percent moisture by volume (field moisture) and dry bulk density were calculated using final oven-dry weight, initial weight and the sample volume. For all calculations, the density of water was assumed to be 1 g cm^{-3}. Dried samples were prepared for further physical and chemical analyses by passing the fine-earth component through a 2.0 mm sieve. The coarse (> 2.0 mm) fraction

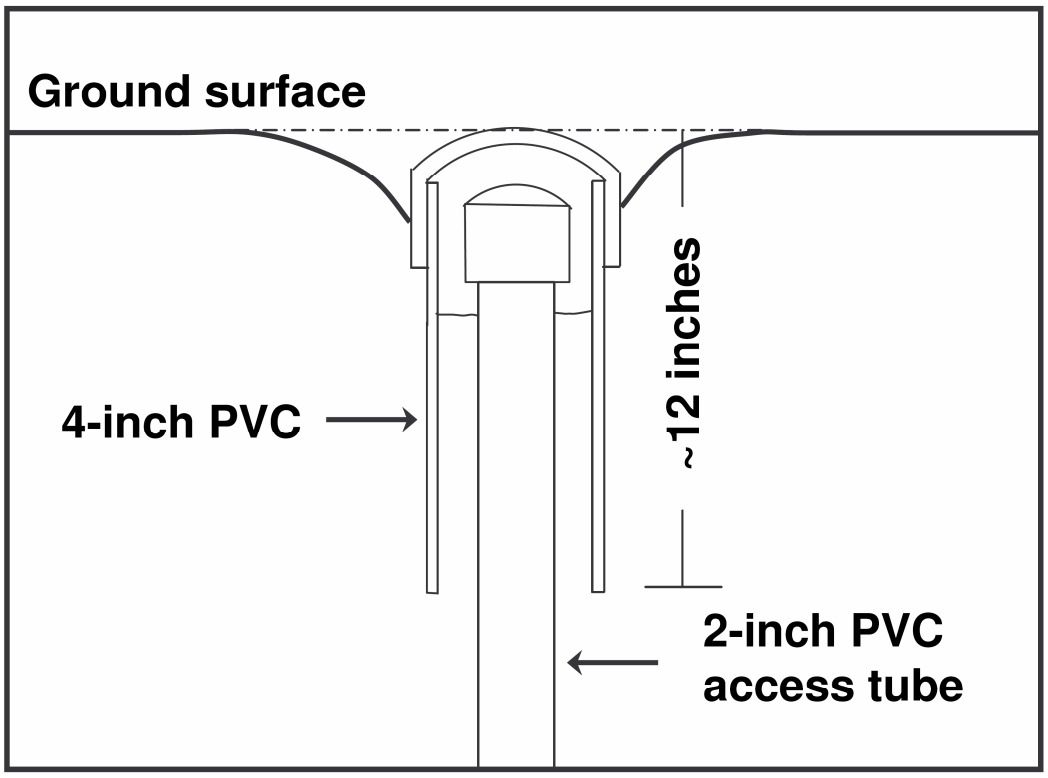

Figure 2.2 Access-tube completion and protection
Diagram showing how access-tubes are completed after installation. A four-inch PVC pipe and end cap protects the top of the access-tube from farm equipment and animals while minimizing interference with natural infiltration around the access-tube.

remaining was weighed and recorded as gravel. The fine-earth portion was mixed and retained for particle size analysis (PSA).

PSAs were performed on each sample using the ASTM 152H hydrometer method using a procedure slightly modified from the method described in Dane (2002). Modifications consisted of collecting hydrometer and temperature readings at intervals of 1, 5, 15, 30, 60, 180, 240, ~480 and ~1,440 minutes. Each hydrometer reading was corrected for the temperature recorded at the time of measurement. This eliminated the need for thermal equilibration in a sedimentation cabinet or temperature controlled water bath. Temperature variations were very small in our lab environment during these measurements. Each PSA used 40.00 g of oven-dried (105°C) $\leq$2.0 mm soil. Percent clay was calculated by plotting the percent of sediment in suspension at each time vs. the log of particle size in microns. For each sample, the equation from a best-fit regression line was used to calculate the amount of clay in each sample. Assuming that clay is composed of all sediments $\leq$ 2 µm, percent clay in suspension is calculated by substituting 2 for particle size in the regression equation.

Percent sand was measured by thoroughly washing each sample through a 53 µm sieve and drying the retained sand at 105°C. The dried sediments were shaken on the sieve to remove any remaining silt or clay. The sand fraction was then weighed and recorded. Percent silt was calculated by difference from the initial 40.0 g sample of $\leq$2.0 mm material.

Traditional PSAs do not measure sand, silt and clay percentages as portions of a bulk soil volume, but instead as a portion of the fine-earth ($\leq$ 2.0 mm) component only. After performing PSAs, we adjusted the percentages of each particle size fraction to include the percentage of gravel measured in the bulk sample. The weight of gravel (> 2.0 mm particles) was recorded when each bulk sample was passed through a 2.0 mm sieve. We chose to include percent gravel in our PSAs because higher rock and gravel content will significantly decrease the bulk dielectric constant and therefore influence the TDR measured moisture content.

A split of each sample was analyzed for standard soil chemical parameters, including pH, BpH (buffer pH, a measure of a soil's natural buffering capacity), acidity, base saturation, Ca

saturation, Mg saturation, K saturation, estimated Cation Exchange Capacity (CEC), total soluble salts (TSS), organic matter (by loss on ignition), and the following extractable nutrients: P, K, Ca, Mg, Zn, Mn, Cu, Fe, and B. Analyses were performed by the Virginia Tech Soil Testing and Plant Analysis Laboratory using the methods described in Mullins (2005).

Statistical analysis

We examined the relationship between TDR moisture readings and actual moisture content using two different regression models. In the first model, we predicted true field moisture using TDR moisture readings and a number of other continuous variables that specify the physical and chemical properties of each sample. This is a standard multiple linear regression (MLR) model which uses the observed numeric values for all of the significant variables in each sample to derive the best estimate of the true moisture content in each respective sample. In this type of regression model the null hypothesis for each possible explanatory variable is that it is not useful in predicting true field moisture. Each variable is treated identically and its importance or lack thereof in the model does not change the interpretation of other variables' importance in the final model.

The second model we used is another type of MLR which uses categorical variables (rather than continuous variables). This method is called categorical linear regression (CLR) and is sometimes referred to as a parallel lines model (Ramsey and Schafer, 1997). In contrast with MLR, a CLR model focuses primarily on the linear relationship between TDR moisture readings and true moisture content within specific categories of physical and chemical parameters. This is done by converting each of the physical and chemical property variables to a categorical variable. The categories we developed for each of the pertinent variables were based on knowledge of how each factor affects the accuracy of TDR moisture readings and represent a defined range of values for each parameter. For example, we divided percent clay into four categories of <15%, 15 to <30%, 30 to <45%, and $\geq$45%. This variable conversion allows us to use TDR readings to predict actual moisture within small, relatively homogeneous subsets of the data. If TDR moisture is significant in explaining field moisture in this model, then the null hypothesis for each of the other categories is that the relationship between TDR moisture and field moisture is the same in that category subset as it is in the baseline category for that variable.

Using the first model, a basic MLR calibration equation for TDR moisture readings was derived using the following statistical analysis software packages: SAS software for general statistical analysis, Analyse-it for graphing and general statistical analysis, and SAS-JMP software for cross-correlation analysis (Analyse-it, Analyse-it for Microsoft Excel; JMP, 1989-2005; SAS, 2000-2004). Prior to MLR modeling, Pearson correlation coefficients and cross correlation plots were used to eliminate from the model variables that showed significant correlation with other variables. Additionally, nearly all chemical parameters are log-normally distributed and were log transformed prior to statistical analysis. Forward, backward and stepwise MLR analysis procedures were used to determine significant variables with a p-value of <0.05. This list was refined to include the fewest variables possible by retaining only those which, when included in the regression model, contributed significantly to the final R^2 value and are most commonly obtained during soil analyses. The same software packages were used in developing and refining the CLR model.

A few statistical outliers were removed from the data prior to development of a final model. These points were identified by examining the distribution of residuals and removing data which were more than 4 standard deviations from the mean. Additional data were removed prior to regression modeling because of known measurement errors due to installation problems of one access-tube. Other points were removed if they were known to be associated with very small soil samples obtained in very cobbly intervals where the true sample volume was highly uncertain and the corresponding TDR measurement was almost certainly affected by surrounding large cobbles. These cobbles are generally not represented in the PSA for a soil sample because they were too large to be sampled. As a result, their effect can not easily be considered in statistical models.

Error analysis

Propagation of measurement errors is useful for understanding how well a statistical model can reasonably fit the data. This prevents over-fitting of the data by addition of more variables than are needed. An error analysis was performed for all variables we used in both statistical models. Because CLR is a type of MLR, equation (2) can be used to estimate propagated errors in both

CLR and MLR models. We modified a standard model of fractional error to derive an equation which propagates errors weighted using the mean parameter value and the regression coefficient:

$$\delta X = \sqrt{(\delta a\,\mu_a\eta_a)^2 + (\delta b\,\mu_b\eta_b)^2 + \cdots + (\delta n\,\mu_n\eta_n)^2} \qquad (2)$$

Where μ_n represents the mean of a variable used and η_n represents the regression coefficient for that variable.

Estimating errors can be challenging because many instruments and methods do not have well-defined errors associated with them. In all cases we use either a stated ± value or our own estimate of measurement error and assume that these values represent one standard deviation from the median measurement for that parameter.

Random errors also occur due to the heterogeneous conditions at our field site. For example, significant errors can result from proximity of the TDR probe to undetected large cobbles, bedrock or small natural voids during measurement. These errors can not be quantified and there is no way of knowing which readings are affected by these factors. As a result, they are assumed to be randomly distributed. These errors should express themselves as a standard deviation of the residuals for the regressed data that is higher than the standard deviation estimated through measurement of error propagation. These residuals should also be normally distributed.

RESULTS

Table 2.1 summarizes the physical and chemical characteristics of the soil samples collected for our study. We compared the mean, range, and standard deviation of values for parameters obtained from soils in sinkhole #1 and sinkhole #5 to broadly examine differences in physical and chemical properties between the two sites. The most significant differences between data shown for sinkholes #1 and #5 in **Table 2.1** were that sinkhole #5 has finer-grained soils (more clay and silt), higher CEC, and contains higher levels of Ca and Mg. Higher extractable Ca and Mg reflect the fact that most access-tubes in sinkhole #5 were augered to bedrock where soils contain significant amounts of weathered carbonates. In sinkhole #1, none of the access-tubes

reached bedrock and none of the samples contained weathered carbonates. Dominantly fluvial sediments are likely the reason for the generally coarser-grained soils sampled in sinkhole #1.

Our particle size analyses placed soil samples within eight of the 12 soil textures as defined by the USDA NRCS (Schoeneberger, 2002), with most being clay and/or silt dominated (**Figure 2.3**). Samples from sinkhole #5 tend to have higher clay and silt content than those in sinkhole #1 and correspondingly lower sand and gravel content. Bulk density values average 1.42 g cm^{-3} for all samples and show no correlation with depth in either sinkhole. This was not unexpected as soil profiles in similar clay-rich soils have also been shown to have approximately constant or decreasing bulk density values with depth (Kool et al., 1986). In many soils, bulk density tends to increase with depth as a result of compaction. In clay-rich soils, this trend can be significantly reduced or not observed at all.

Multiple linear regression

A simple linear regression of TDR moisture values against measured field moisture values produced an R^2 statistic of 0.23 (**Figure 2.4**a), indicating that there is not a simple linear relationship between TDR moisture measurements and field moisture values. Furthermore, non-linear trends were not visible in the data and other models (such as polynomial or exponential) did not result in a better relationship. For this case, and with a large set of physical and chemical parameters potentially affecting the TDR moisture versus field moisture relationship, MLR analysis was a more appropriate method than simple linear regression. Normal distribution of standardized residuals is another important test of whether linear regression models are appropriate. **Figure 2.5** shows normal distribution of standardized residuals, indicating that MLR models are suitable for all three data sets. If this were not the case, either non-linear regression techniques should be used or the data must be transformed prior to regression.

For the MLR model, data were analyzed both as a single group and divided by study sinkhole into two groups. Pearson cross-correlation statistics and cross-correlation plots were constructed to identify parameters that should be removed from the variable set or not included if a related parameter is included. For example, because the percentages of gravel, sand, silt and

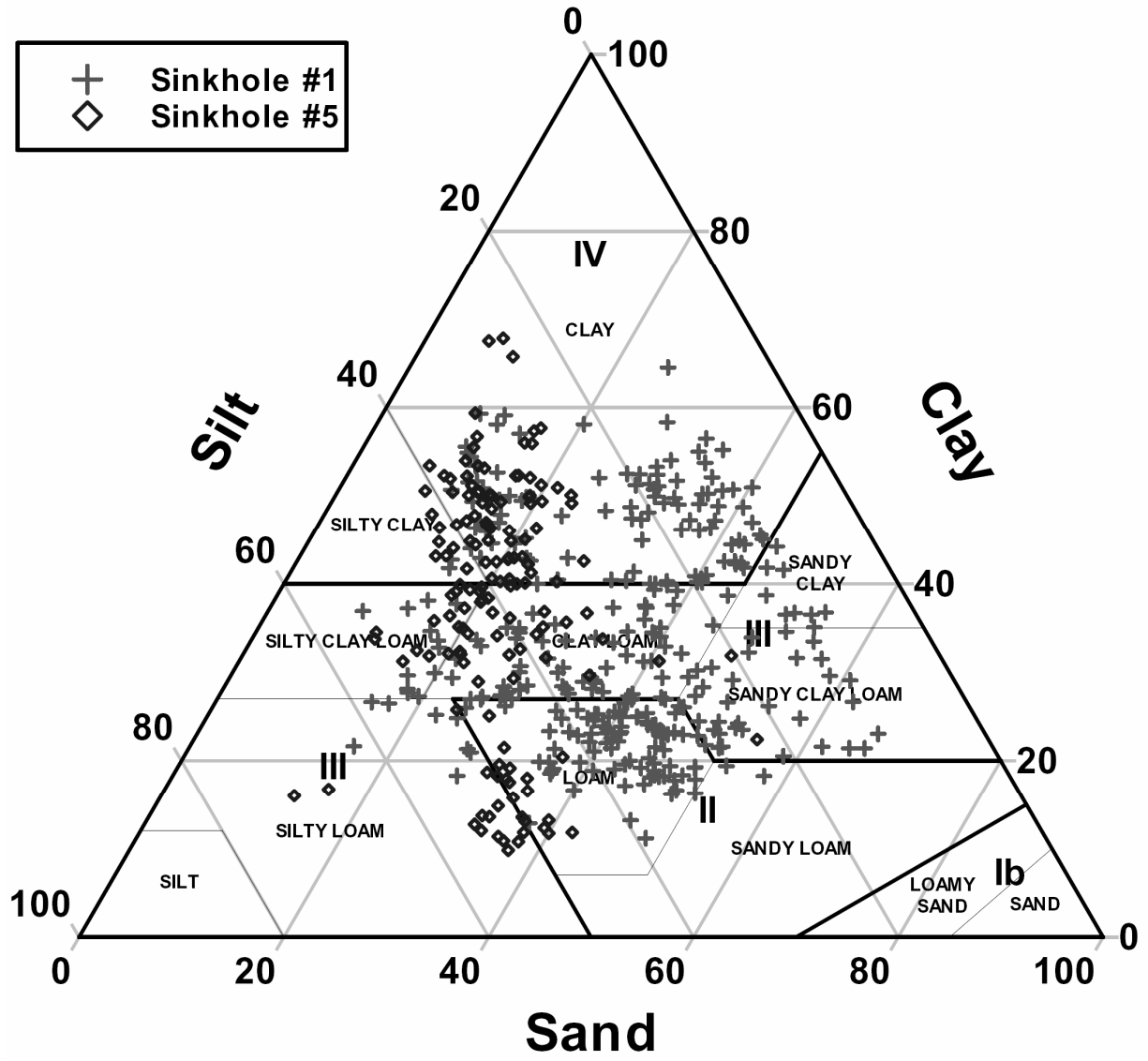

Figure 2.3 USDA soil texture with all samples plotted

Soil classification diagram showing the heterogeneity in USDA soil textural properties for samples collected in both sinkholes. Crosses [+] are from sinkhole #1 and diamonds [◊] are samples from sinkhole #5.

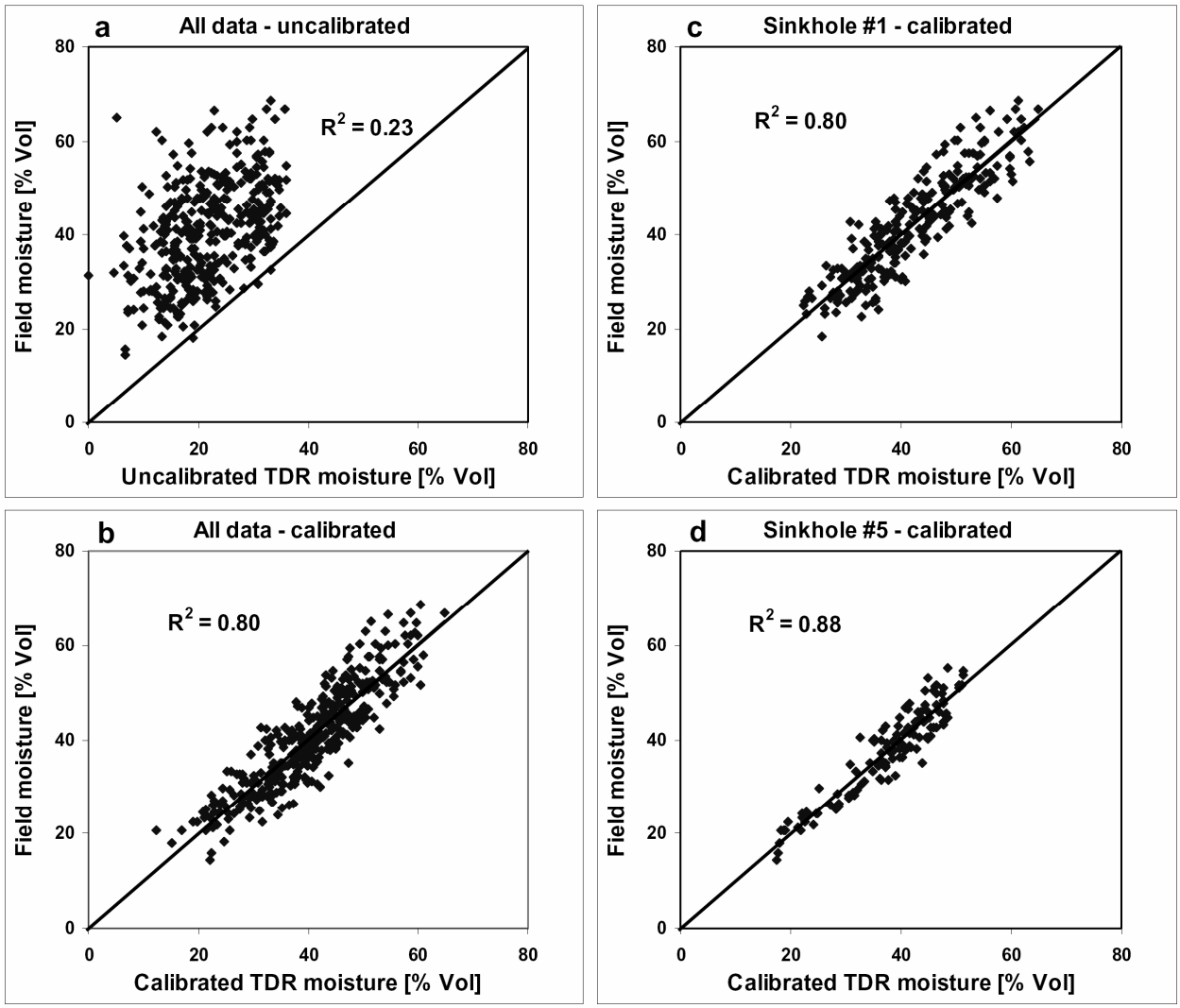

Figure 2.4 Plot of calibration fits using MLR

Diagrams showing: a) un-calibrated TDR moisture readings vs. laboratory-measured field moisture values, b) all calibrated data vs. field moisture, c) calibrated data for sinkhole #1 vs. field moisture, and d) calibrated data for sinkhole #5 vs. field moisture. Diagonal lines represent a 1:1 relationship between calibrated TDR values and field moisture.

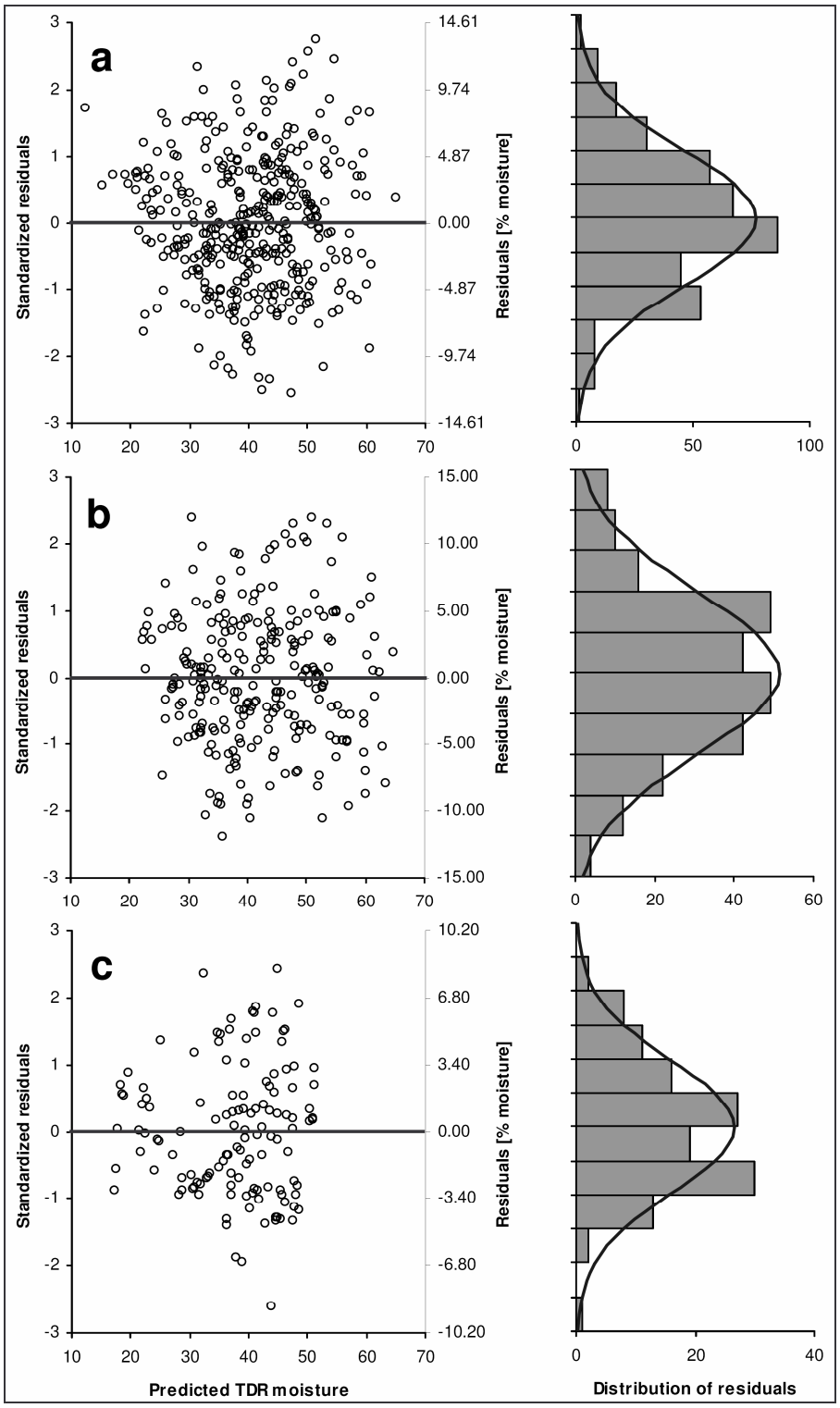

Figure 2.5 Distribution of residuals for MLR results
Distribution of standardized residuals for a) all data, b) sinkhole #1, and c) sinkhole #5. Left plots show distribution of residuals in standardized units (left axis) as well as % moisture (right axis). Right plots show a frequency histogram with a normal distribution curve.

clay sum to 100% for each sample, they should not be simultaneously included in the regression model. MLR was then used to obtain baseline calibration results using TDR moisture and key physical and chemical soil parameters. Common variables included in MLR models for all three groups of data are: TDR moisture, percent clay, depth, percent silt, bulk density, estimated Cation Exchange Capacity (CEC), and log of % calcium saturation (**Table 2.2**). Of these six variables, percent clay and depth explained much of the difference between TDR readings and measured field moisture. Inclusion of these two variables alone increased the R^2 statistic to approximately 80% of the final R^2 value for each model.

Percent clay affects TDR moisture values due to the fact that water molecules bound between clay particles of certain mineralogies tend to be less responsive to TDR measurement (Sabburg et al., 1997), which decreases the bulk dielectric constant, thereby decreasing the resulting TDR moisture value. In essence, the bound water molecules are not able to freely move and interact with the electromagnetic pulse produced by the TDR probe during measurement, thereby limiting the ability of the probe to detect the bound water. This is reflected in our data by positive regression coefficients for percent clay (**Table 2.2**).

The influence of installation depth on TDR-moisture values is important to recognize and estimate when using access-tube style TDR probes. This has been recognized by other researchers (Whalley et al., 2004) who concluded that near-surface disturbances of soil structure were caused by access-tube installation. The disturbances resulted in increased air gaps and air-filled fractures, which decreased the bulk dielectric constant. In our study, repeated insertion and extraction of an auger, no matter how carefully it was done, inevitably led to slight borehole enlargement (especially at or near the surface) and possible soil structure disturbances. Both factors effectively reduce the bulk dielectric constant by introducing air gaps around the access-tube. At greater depths, these factors and related effects are greatly reduced because of fewer disturbances related to augering. However, when we examined the effect depth has on our TDR moisture readings we observed the opposite effect. Instead of the negative correlation found by Whalley, et al (2004), (indicating the influence of air gaps and increased soil disturbances near the surface), we found a strong positive correlation with depth (**Table 2.2**). Although this is good evidence that our access-tube installation methods do not affect TDR measurements, we are

not yet able to fully explain the reasons for this relationship and leave this topic open for further investigation. A possible explanation is that the amount of water bound by various clay minerals is increasing with depth. Moisture content increased systematically with depth in moisture profiles.

Estimated CEC was included in our MLR model because an increase in CEC increases the bulk dielectric constant (Garrouch and Sharma, 1994). This results in increased TDR moisture values, which is reflected by the negative coefficient for CEC values in our calibration equations. The log of percent calcium saturation was included in the model because of its statistical significance and because calcium concentration has also been shown to affect TDR readings (Vogeler, 2001) by increasing the bulk dielectric constant. This is again reflected by the negative correlation coefficient (**Table 2.2**).

Because bulk density is related to mineral grain properties and porosity, there is a theoretical basis for its effect on the bulk dielectric constant (Roth et al., 1990). While bulk density had a relatively small influence on TDR moisture values in our work, we included it in our calibration model because it is statistically significant and is a parameter which is relatively easy to measure. Other field-based studies have shown similar results where bulk density had little or no influence on TDR readings (Whalley et al., 2004). Even some lab-based research has shown relatively insignificant effects of bulk density on bulk dielectric constant (Jacobsen and Schjonning, 1993). The reason for the relative insignificance of bulk density in field conditions and in certain lab experiments, when theoretical and some lab work indicate the opposite should be true, is the subject of debate and one that has not yet been resolved in the literature.

In addition to analyzing the data as a single set and divided by study sinkhole (**Table 2.2**), we also performed MLR analyses on data sets grouped by soil texture (results not shown). In some cases better fits were obtained using this method while in other cases poorer fits were achieved. In most cases fewer variables were required to obtain a final regression model. Because there was not an overall improvement in calibration results, and our soils are highly heterogeneous with respect to physical and chemical properties, we have chosen to use the entire data set and only divide it with respect to sinkhole. This is justified because the sinkholes sampled are

widely separated and are formed in river terraces of different ages and composition. It also allowed us to compare differences between the two sinkholes and the entire data set.

Regression statistics for three baseline MLR calibration models which include the same parameters in each model are presented in **Table 2.2**. With the exception of TDR moisture, p-values of <0.005 indicate that all variables are significant. From the results of the MLR analysis, we derived the baseline calibration equations (3), (4) and (5) for each data set using regression coefficients for each parameter.

For the entire data set:

$$\Theta = \left(0.053 - \left(0.062 \cdot \theta TDR\right) + \left(0.881 \cdot C\right) - \left(0.609 \cdot D\right) + \left(0.442 \cdot S\right) + \left(8.542 \cdot \sigma_b\right) - \left(2.988 \cdot CEC\right) - \left(7.210 \cdot \log Ca\right)\right) \quad (3)$$

For sinkhole #1:

$$\Theta = \left(0.921 - \left(0.102 \cdot \theta TDR\right) + \left(0.917 \cdot C\right) - \left(0.621 \cdot D\right) + \left(0.439 \cdot S\right) + \left(5.206 \cdot \sigma_b\right) - \left(2.806 \cdot CEC\right) - \left(4.282 \cdot \log Ca\right)\right) \quad (4)$$

For Sinkhole #5:

$$\Theta = \left(7.879 + \left(0.045 \cdot \theta TDR\right) + \left(0.627 \cdot C\right) - \left(0.508 \cdot D\right) + \left(0.291 \cdot S\right) + \left(14.235 \cdot \sigma_b\right) - \left(1.347 \cdot CEC\right) - \left(14.361 \cdot \log Ca\right)\right) \quad (5)$$

Where Θ = baseline calibrated soil moisture *[%]*, θTDR = TDR moisture *[%]*, C = percent clay, D = depth [ft], S = percent silt, σ_b = bulk density [g/cm^3], CEC = Cation Exchange Capacity [meq/100g], and $log\ Ca$ = log of percent calcium saturation [%]**.** Equation (3) is the baseline calibration equation for the entire data set, (4) is for data from sinkhole #1 and (5) is for data from sinkhole #5. It is important to note that the coefficients in these calibration equations are specific only to this instrument which contains an internal factory-set standard calibration equation. Knowing the instrument's internal calibration is not important for obtaining a secondary calibration equation using our methods. It is, however, important that internal calibrations not be changed during subsequent calibration and data collection work. If our results are used to calibrate other's TDR measurements without performing a similar statistical analysis, care should be taken to understand the relationship between our calibration equations (3, 4, and 5) and the TDR moisture measurement's relationship to the pseudo transit-time equation (1). **Figure 2.6** shows a vertical moisture profile of uncalibrated and calibrated moisture content compared with gravimetrically measured soil moisture.

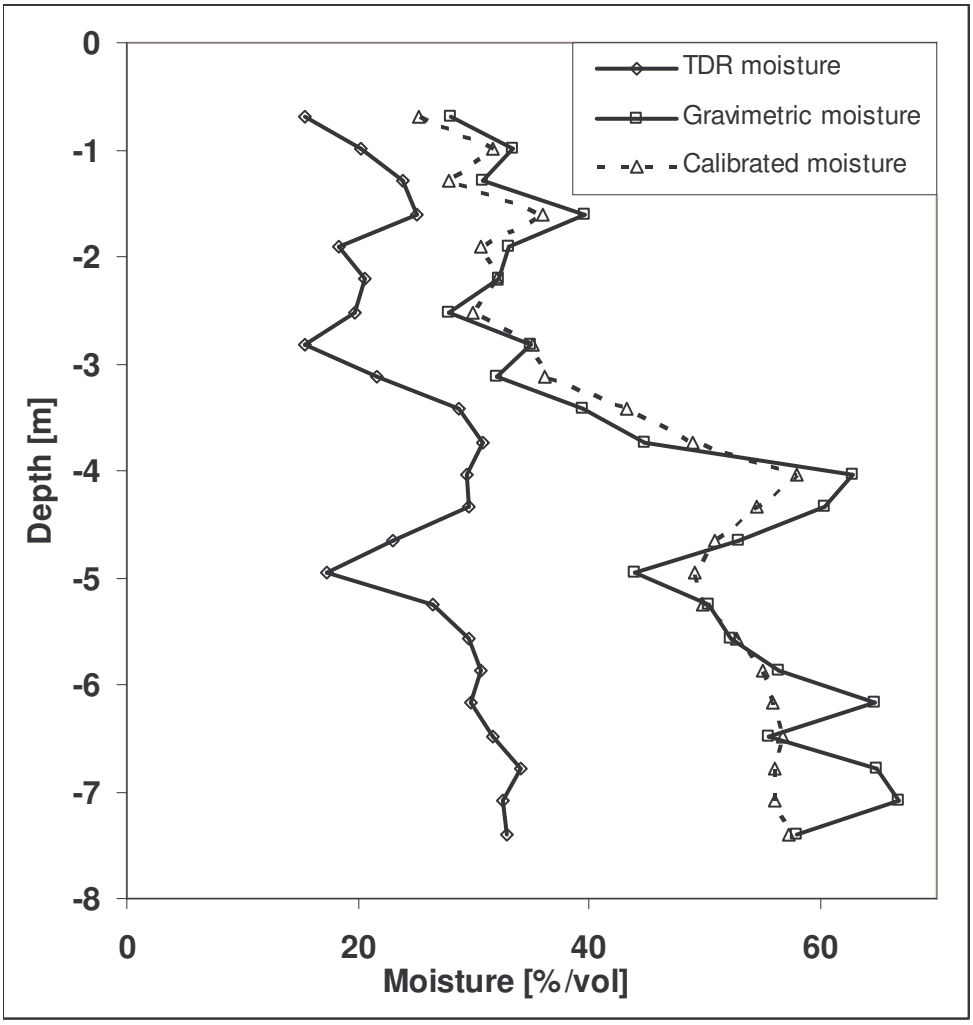

Figure 2.6 Comparison of TDR, gravimetric, and calibrated TDR soil moisture. Figure showing an example of a 1-dimensional moisture profile with depth. Solid line with diamonds represents uncalibrated TDR moisture, solid line with squares represents gravimetrically measured soil moisture, and dashed line represents the MLR-model calibrated TDR moisture.

Figure 2.7a, b and **c** show how the R^2 statistic increases as the standard deviation of residuals decreases with inclusion of additional variables in the MLR calibration model. Both the R^2 and the standard deviation were important criteria in choosing the number of parameters we kept in our final models. Sequential addition of TDR moisture, % clay, depth, % silt, bulk density, CEC, and log % Ca saturation did not increase the R^2 statistic more than 0.015 per variable added. Because the standard deviation of residuals is not less than the weighted propagated error estimate in each model (shown by the horizontal lines in **Figure 2.7**), we conclude that we have not included more parameters than are reasonable in the regression model and have not over-fitted the model.

Figure 2.4 (**b, c** and **d**) illustrates the improved fit of calibrated TDR moisture data using our final calibration equations compared to un-calibrated data (**Figure 2.4a**). Compared to the R^2 of 0.23 for uncalibrated TDR moisture *vs.* field moisture, the R^2 values are: for all data, 0.80; for sinkhole #5, 0.88; for sinkhole #1, 0.80.

Categorical linear regression (CLR)

CLR modeling produced results that are very similar to MLR results, though TDR moisture is more significant in the categorical model and the coefficient for TDR moisture is larger (**Table 2.3**). This result indicates that there is a slightly stronger relationship between TDR moisture and the measured field moisture than is shown using MLR. Although the results show TDR moisture has more influence on the final calibrated data than in MLR, the coefficient for TDR moisture is still small. As with the MLR results, this supports the idea that access-tube TDR measurements are measuring 'free' moisture and the difference between TDR moisture and field moisture is primarily due to the effects of chemical and physical soil properties. The results of our CLR modeling are shown in **Table 2.3** and **Figure 2.8** Fit and residual distribution for CLR results . The baseline calibrated fit for all data points using CLR is very similar to that achieved with MLR. The R^2 statistic is 0.75 *vs.* 0.80 and residuals are normally distributed (**Figure 2.8** Fit and residual distribution for CLR results).

The baseline CLR model includes 7 categorical variables other than TDR moisture which are statistically significant ($Pr > |t| \leq 0.05$): depth, % clay, % sand, bulk density, log Ca saturation,

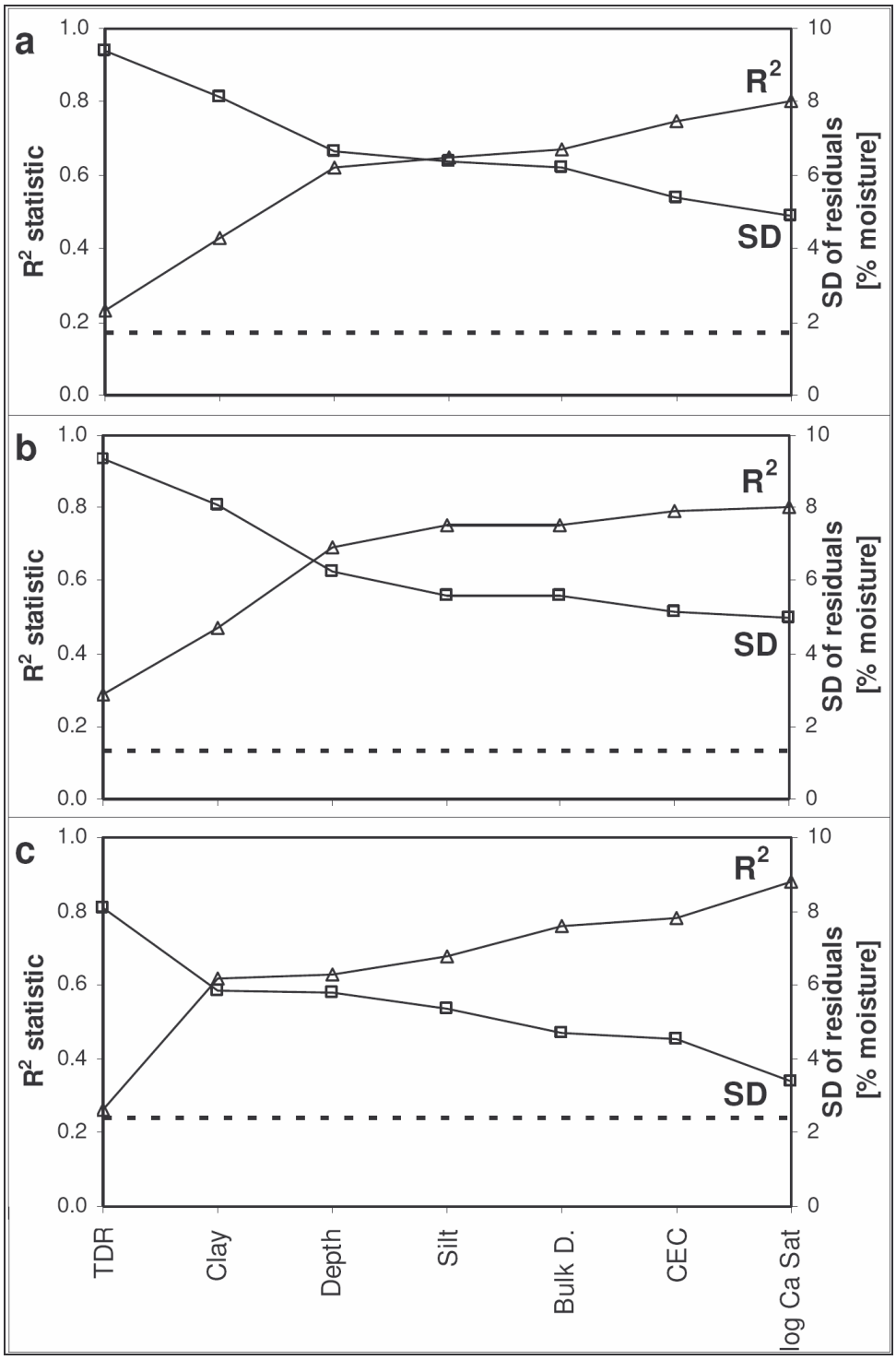

Figure 2.7 Change in MLR calibration fit with additional variables
Diagrams showing for a) complete data set, b) sinkhole #1, and c) sinkhole #5, how regression statistics increase (triangles) and the standard deviation of moisture residuals (squares) decrease with addition of variables. Lower horizontal dashed lines in each plot indicate weighted propagated error estimates based on the relative influence of each variable in the regression model.

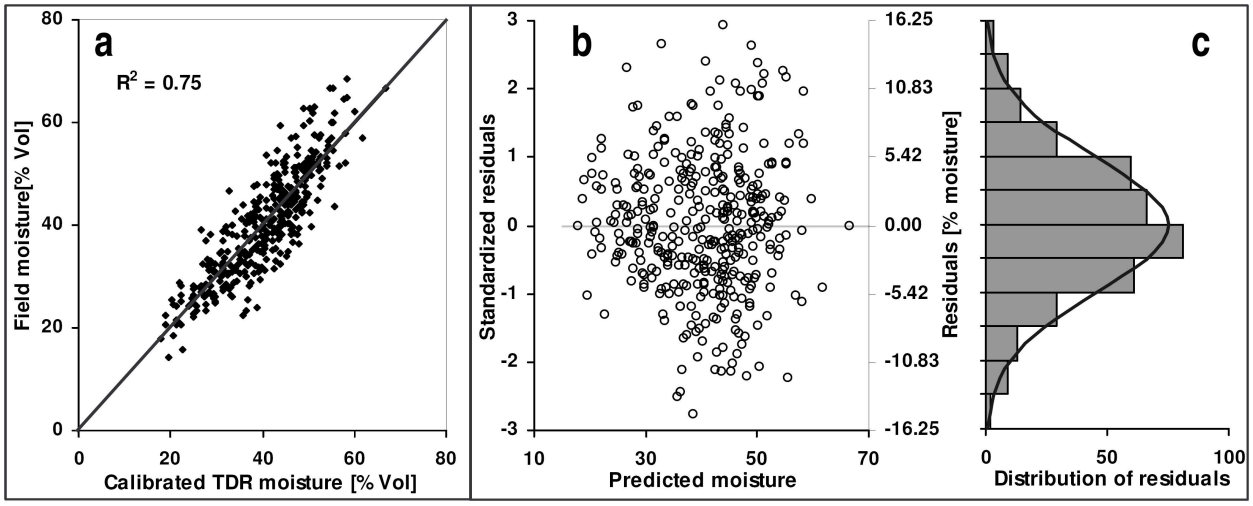

Figure 2.8 Fit and residual distribution for CLR results

Diagram showing field moisture values *vs.* calibrated TDR moisture values resulting from the categorical regression model a). Plots b) and c) show standardized residuals and residual distribution for the categorical regression model.

estimated CEC, and % organic matter. These are the same variables that were significant in the MLR model except that % sand is included instead of % silt in the CLR model (because of greater significance), and % organic matter is significant enough to include in the CLR model. Organic matter has been shown to have effects similar to those of clay on the bulk dielectric constant (Jacobsen and Schjonning, 1993), which is shown in our CLR results by positive parameter estimates for both variables (**Table 2.3**).

The baseline CLR calibration method differs slightly from the MLR method which uses a single linear equation for all data included in the model. In CLR results, each category is matched with a parameter estimate. Parameter estimates for each category are summed to obtain a calibrated moisture value. As an example, to calculate a baseline calibrated moisture value for a sample with the following parameter values (TDR moisture = 15.4, depth = 2.25, % clay = 13.14, % sand = 47.02, bulk density = 1.52, log Ca Sat = 1.73, CEC = 2.5, % organic matter = 1), each parameter is first assigned a category. Using our categories and regression results presented in **Table 2.3**, the baseline calibrated moisture value (Θ) is calculated by summing the following: [27.39 (intercept term) + (0.214 x 15.4) (TDR term) + 0 + 0 - 9.11 + 3.47 - 7.03 + 0 + 4.10]. Using parameter estimates in the same order as listed above, this produces a baseline calibrated moisture value of 22.13%. Zero values represent parameter estimates for data within a baseline category and are included as place-holders in this example. Non-zero parameter estimates represent differences between the relationship within a category and the corresponding baseline category.

Although it would be difficult to show all the categorical subsets specified in the model, we use two of the more important variables in an example which illustrates the essential benefit of the CLR approach. **Figure 2.9** Relationships between variables using CLR shows the relationship between TDR moisture readings and field moisture values in each of the depth and percent clay category subsets. This figure shows both the observed data and the estimated regression relationship each in subset. Although the regression lines shown are not parallel, our model analyses found that an additional model term allowing these slopes to be distinctly defined for each category was insignificant.

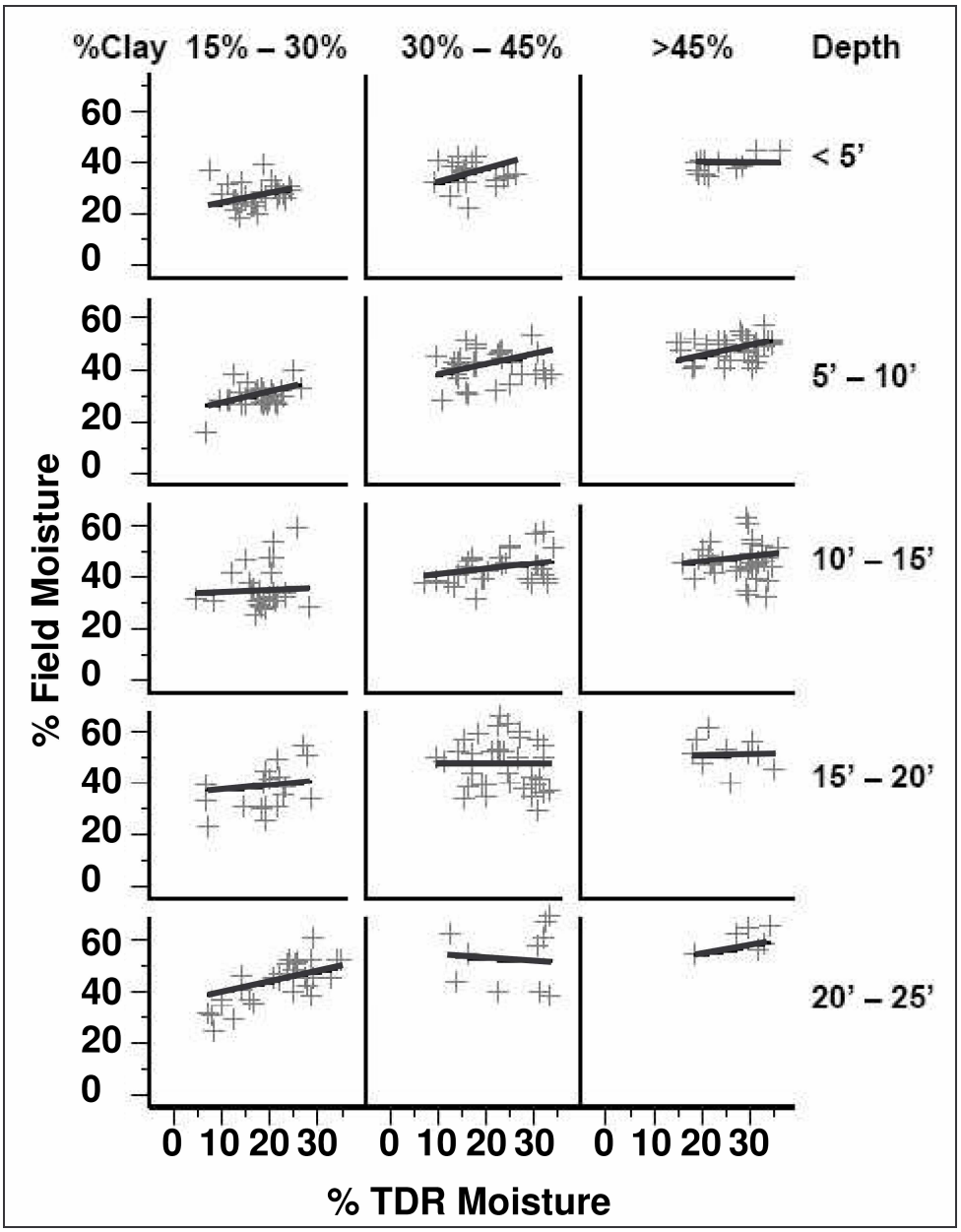

Figure 2.9 Relationships between variables using CLR
Diagram showing the relationship between TDR moisture and field moisture within each of the depth and percent clay category subsets. The lowest category for percent clay and the deepest category for depth have both been excluded because they contained either no or very few observations (<5 obs.). Actual observations are indicated by grey [+] symbols. The regression relationship between TDR moisture and field moisture in each subset is illustrated by the black lines.

Effects of bound water on TRIME TDR moisture readings

The fact that TDR moisture had low significance in the derivation of the baseline calibration equation was surprising as we expected there to be a much stronger relationship between TDR moisture and field moisture. The lack of a strong relationship indicates that the difference between TDR moisture readings and gravimetric soil moisture is the result of something other than a systematic error in the factory calibration. An alternate explanation for the insignificance of TDR moisture in the regression models is that the range of moisture values measured for each soil texture is somewhat limited. Increasing the range of moisture values measured in each texture may have revealed a stronger relationship, but we were not able to investigate this possibility as we were limited by field conditions.

Perhaps the most important implication of TDR moisture having low significance in the regression models is that the measured TDR moisture content is an accurate measurement of the 'free' water in open pores and that the difference between TDR moisture and field moisture is dominantly due to physical properties of the soil controlling the bound water content which is undetectable by the TDR probe. To a lesser extent, the difference is also influenced by chemical effects on the bulk dielectric constant. As a result, any calibration to correct for this difference would not be influenced by the measured TDR moisture. This is a logical assumption since the TDR probe is designed and calibrated at the factory to measure this 'free' fraction of moisture in a soil and is not calibrated to correctly measure moisture in soils with high clay content or high salinity. With this in mind it becomes clear that, in certain soils, TDR moisture measurements may only be useful for measuring and monitoring changes in this 'free' moisture; a point which is not widely discussed in the literature. The remaining bound moisture can reasonably be assumed to remain constant in deep soil profiles where the influence of evapotranspiration is minimal.

Calibrating time-series TDR measurements after baseline calibration is established

Regression modeling indicated that the difference between θTDR and gravimetrically measured soil moisture can almost entirely be explained by the effects of the physical and chemical parameters of the soil. Because θTDR had little influence on the baseline calibrated moisture

values, changes in θTDR observed after the very first measurement (θTDR_i, which was used to develop the baseline calibration) can be interpreted to primarily represent changes in the 'free' moisture content. Using this rationale, our model for calibrating subsequent θTDR measurements (θTDR_t) obtained at the same point is relatively simple and consists of adding the measured change in θTDR ($\theta TDR_t - \theta TDR_i$) to the baseline calibrated value (Θ).

As an example, consider the initial uncalibrated TDR measurement (θTDR_i) which was collected immediately after access tube installation, and a subsequent TDR measurement (θTDR_t) obtained at time t. The baseline calibration equation is applied to θTDR_i to obtain the baseline calibrated moisture content (Θ). The calibrated moisture value at some time t (Θ_t) for the measurement θTDR_t is obtained by adding the difference between the subsequent and initial θTDR measurements to Θ:

$$\Theta_t = \Theta + (\theta TDR_t - \theta TDR_i) \quad (6)$$

DISCUSSION

Calibration of TDR measurements

Determining how physical and chemical parameters can explain the difference between field TDR moisture measurements and gravimetric moisture measurements from soil samples was the primary objective of this study. We believe that equation (3) represents a general calibration equation that can be used to adjust TRIME T3-50 IPH TDR moisture measurements when the required physical and chemical soil parameters are also measured. Calibrated values for subsequent TDR measurements at the same location can then obtained by applying equation (6). Although we believe that our results are broadly applicable, the effects of certain physical and chemical parameters on soil moisture should be evaluated at individual field sites to obtain the most accurate soil moisture measurements. As an example, this is especially true if the clay mineralogy is significantly different, as clay minerals have widely variable capacities for bound water.

Our results highlight parameters which best explain differences between field moisture and TDR measurements in all three data sets, using two regression methods. They also emphasize that instrument-programmed material-specific calibration equations will not produce accurate results

in heterogeneous soil profiles. Our baseline calibration methods are, in essence, a material specific calibration for each TDR measurement. In equation (3), coefficients represent the results of using MLR on the larger set of 383 samples. While the coefficients for equations (4) and (5) are somewhat different from equation (3), the values are similar and tend to bracket the coefficients in equation (3). This supports the idea that, for this TDR instrument, equation (3) is a general MLR calibration model suitable for use in texturally heterogeneous soils with similar chemical properties.

The CLR results can also be used as a general calibration method. We chose to model the data using CLR and include the results because CLR emphasizes different relationships within the data. For example, in MLR, the relationship between TDR moisture and field moisture is not emphasized and can be diminished by stronger relationships between other variables in the model. Using a CLR model allowed us to emphasize the relationship between TDR moisture and field moisture while examining it over the ranges (which are divided into categories) of each additional variable. Results of the CLR model corroborate the results of our MLR modeling and support the notion that discrepancies between gravimetrically measured TDR moisture are not detected using a factory installed calibration equation. The amount of bound, or undetectable, water in our soils is controlled almost entirely by physical and chemical parameters.

Our results can be used as a guide for evaluating the relative importance of soil parameters when performing similar calibration work in the future. The first four parameters (% clay, depth, % silt, and bulk density) are relatively easy to obtain during basic physical characterization of a soil sample and, depending on the goals of a study using access-tube TDR, may provide an acceptable initial calibration. Aside from depth, these parameters are related to soil texture and the associated dielectric properties of mineral grains, porosity, and the effects of bound water in clays. Adding additional parameters such as CEC and log % Ca saturation (which are easily obtained with a routine soil chemical analysis) allows some of the more important dielectric effects of soil chemistry to also be incorporated in the model.

Because a standard soil chemical analysis usually measures many parameters, rather than specific parameters such as CEC and % Ca saturation, using the additional parameters in

regression modeling is easy and economical. We investigated how additional chemical parameters might further improve our regression models. Results indicated that additional parameters did improve the calibration fit by small but statistically significant increments for each group of data. Parameters which were significant (at p-values of <.005) in one or more of the models were pH, log Mn, Organic Matter, and log % K saturation. Ultimately, we decided that inclusion of these parameters was not justified because of relatively small increases in R^2 values (.01 to .015 per parameter) or because of indications that cross-correlation may be a problem. For example, pH and log Ca saturation have a Pearson correlation coefficient of 0.75. However, these results indicate that many other chemical factors are subtly influencing TDR measurements and, depending on the situation, may deserve inclusion in a final regression model. This is not surprising considering that many chemical parameters can alter the dielectric properties of the pore waters being measured.

The accuracy of our baseline calibration models varies depending on data grouping (all data *vs.* division by sinkhole). This is likely the result of differences in random error distribution in TDR measurements that can not be quantified such as proximity of the probe to cobbles or natural voids. Measurements made in soils with more undetected cobbles would result in larger variability in the regressed data. This is supported in our data by the fact that sinkhole #1 contained the most cobbles encountered and also has the highest residual variability in the calibrated moisture values. The results of our baseline MLR models predict a one standard-deviation accuracy of ±4.87, ±5.00 and ±3.40% in volumetric moisture for (3), (4) and (5), respectively. With the CLR model, one standard-deviation in residuals is $\pm$5.42% in volumetric soil moisture. Using our methods, and understanding that random heterogeneities in a field setting will introduce significant variability, we believe that achieving better calibration results is unlikely. For example, achieving an R^2 of 0.99 would not be reasonable considering the natural variability in the system as well as the effects of propagated errors. However, as outlined above, small improvements may be possible by including additional chemical parameters in a regression model.

INSTALLATION

The manufacturer-recommended method for installing TDR access-tubes is to use specialized tools and an auger inside the access-tube to bore a hole approximately the same diameter as the inside of the access tube. Augering is done in short increments and the access tube is then hammered downward from the top (IMKO, 2001). The augered hole is enlarged to the outer diameter of the access-tube as surrounding soils are 'shaved' off by a special cutting head that protects the end of the access-tube. This results in a tight fit between the soil and the tube. In addition to physical limitations on installation depth for this method, there are also practical reasons why it is not suitable for certain soils. Whalley (2004) reported evidence that vibrations from hammering caused significant disturbances in soil structures and probably introduced air gaps around upper portions of the tube. In the clay-rich soils at our field sites and with practice, our method of augering a hole first and then slowly pushing the access-tube into the hole seems to have overcome both of these limitations. Pushing slippery PVC access tubes steadily downward can be quite challenging. We used a long loop of 1-inch tubular nylon climbing webbing as a clamp and a long lever to apply steady downward force on the access-tube. As the tube slid downward, the clamp was moved incrementally upwards and the process repeated until the tube was installed. This method would not be ideal in soils where stability of the augered hole is an issue.

Other researchers have installed access-tubes composed of various plastics as well as fiberglass (Laurent et al., 2005). We used schedule 40, 2.375-inch (6.03 cm) diameter, PVC threaded well-casing access-tubes because they are relatively inexpensive, can be smoothly joined without the need for a connector that increases the outer diameter of the tube, and are sturdy enough to resist damage while applying significant steady force during installation. Additionally, the T3-50 IPH probe is designed for use in schedule 40 PVC pipe. For deep access-tubes, this type of tube and installation method combination seems to be ideal.

Recommended installation methods

Based on our experiences, we suggest the following method for installing access-tubes that will permit accurate TDR measurements at depths up to (and possibly greater than) 30 feet (9.1 m) and will allow subsequent calibration. First, a hole should be augered that is the same diameter

as the access tube. During augering, volumetric soil samples should be collected at intervals that correspond to planned TDR measurement depths. These soil samples can later be used to obtain the parameters used in our MLR and CLR results. Second, the access tube should be installed with careful, steady downward pressure rather than hammering. Last, TDR moisture measurements should be collected immediately after access tube installation.

CONCLUSIONS

Our study shows the importance of calibrating TDR moisture readings to obtain accurate field moisture values from an access-tube instrument in environments where a wide range of soil properties are encountered. To obtain accurate field-moisture values, a large set of soil samples can be characterized and statistically analyzed to determine which parameters significantly influence the bulk dielectric constant of soil. Our baseline MLR calibration model uses TDR moisture, % clay, depth, % silt, bulk density, CEC, and log % Ca saturation to predict an initial field moisture value at each sample point. Minor improvements to the fit of each model were made by adding two or three statistically significant chemical parameters. While these parameters probably do influence the bulk dielectric constant of moist soils, they did not make a large enough difference in our regression results for us to confidently include them in our final MLR models.

Our baseline CLR model uses TDR moisture, depth, % clay, % sand, bulk density, log % Ca saturation, estimated CEC, and % organic matter. As with MLR, minor improvements could be made to the fit of the model, but additional categorical variables did not make large enough differences for us to include them in our final categorical model. The CLR model did not produce significantly different calibration results from the MLR (**Figure 2.8** Fit and residual distribution for CLR results *vs.* **Figure 2.4** and **Figure 2.5**). However, it did reinforce the conclusions reached using MLR, which were that the differences between TDR moisture and field moisture values are primarily the result of effects due to physical and chemical properties.

While TDR calibration for access-tube measurements is a potentially difficult exercise, it can and should be done if TDR will be used to measure soil moisture in heterogeneous soils – especially those with high clay content. We have determined which parameters best explain discrepancies

between access-tube TDR and gravimetrically measured moisture measurements so that others might use this information to design sampling and calibration methodologies in the most time and cost-effective manner.

In our study, un-calibrated access-tube TDR moisture measurements significantly and consistently underestimated true field moisture values (**Figure 2.4a**). In our MLR and CLR model results, TDR moisture has a very small and statistically insignificant effect on initial calibrated moisture values in our analyses (p-values are all > 0.05). This leads us to the conclusion that large differences between measured TDR moisture values and corresponding gravimetrically measured soil moisture values are due to the effects of (dominantly) physical and (to a lesser extent) chemical soil properties on soil moisture which the TDR probe we used is not able to detect.

After a baseline calibration is applied, subsequent TDR measurements in the same location can be calibrated using equation (6). This method assumes that temporal changes in uncalibrated TDR measurements are the result of changes in 'free' soil moisture and that bound moisture remains essentially constant over time in deep profiles, is mostly undetectable by the TDR probe, and is accounted for by using the baseline calibration.

ACKNOWLEDGEMENTS

We would like to acknowledge funding for this research from: US Department of Education GAANN Fellowship, Virginia Water Resources Research Center, Cave Conservancy Foundation, Cave Research Foundation, National Speleological Society, Geological Society of America, West Virginia Association for Cave Studies, and the Virginia Tech Graduate Research Development Program. We would also like to thank Dr. Rolf Becker and Mr. Timo Camek at IMKO for their generous technical assistance and advice. We thank Ankan Basu, Mike Beck, Lee Daniels, Beth Diesel, Bruce Dunlavy, Frank Evans, Brad Foltz, Marty Griffith, Mary Harvey, Ashley Hogan, Danielle Huminicki, Stuart Hyde, Rachel Lauer, Steve Nagle, Jeanette Montrey, Wil Orndorff, Zenah Orndorff, Dave Rugh, Cori and Zachary Schwartz, Jim Spotila, Brett Viar, Dongbo Wang, and Brad White for their assistance both in the field and in the lab.

REFERENCES

Analyse-it for Microsoft Excel. Leeds, UK. See http://www.analyse-it.com/.

Chandler, D.G., M. Seyfried, M. Murdock, and J.P. McNamara. 2004. Field Calibration of Water Content Reflectometers. Soil Science Society of America Journal 68:1501-1507.

Dane, J.H., Topp, G.C., (ed.) 2002. Methods of soil analysis. Part 4: physical methods, pp. 1-1692. Soil Science Society of America, Madison, Wisconsin.

Dobson, M.C., F.T. Ulaby, M.T. Hallikainen, and M.A. El-Rayes. 1985. Microwave dielectric behavior of wet soils - part II: dielectric mixing models. IEEE Transactions on Geoscience and Remote Sensing GE-23:35-46.

Evett, S.R., and J.L. Steiner. 1995. Precision of neutron scattering and capacitance type soil water content gauges from field calibration. Soil Science Society of America Journal 59:961-968.

Garrouch, A.A., and M.M. Sharma. 1994. The influence of clay content, salinity, stress and wettability on the dielectric properties of bring saturated rocks: 10 Hz to 10 MHz. Geophysics 59:909-917.

IMKO. 2001. TRIME-FM User Manual - 22 pgs.

IMKO. 2006a. Micromodultechnik GmbH. Theoretical aspects on measuring moisture using TRIME, Ettlingen, Germany.

IMKO. 2006b. Theoretical aspects on measuring moisture using TRIME - pages 33-55.

Jacobsen, O.H., and P. Schjonning. 1993. A laboratory calibration of time domain reflectometry for soil water measurement including effects of bulk density and texture. Journal of Hydrology:147-157.

1989-2005. Version 6. SAS Institute Inc, Cary, NC.

Kool, J.B., K.A. Albrecht, J.C. Parker, and J.C. Baker. 1986. Physical and chemical characterization of the Groseclose Soil Mapping Unit. Virginia Agricultural Experiment Station Bulletin 86-4:75.

Laurent, J., P. Ruelle, L. Delage, A. Zairi, B.B. Nouna, and T. Adjim. 2005. Monitoring soil water content profiles with a commercial TDR system: comparative field tests and laboratory calibration. Vadose Zone Journal 4:1030-1036.

MESA-Systems. 2006. 50mm Tube Access Probes specifications [Online] http://www.mesasystemsco.com/product.asp?id=6#.

Mullins, G.L., Heckendorn, S. E. 2005. Draft Copy of Laboratory Procedures - Publication 452-881. Virginia Tech Soil Testing Laboratory, Blacksburg.

Ramsey, F.L., and D.W. Schafer. 1997. The statistical sleuth: a course in methods of data analysis. Duxbury Press, Belmont, CA.

Roth, K., R. Schulin, H. Fluhler, and W. Attinger. 1990. Calibration of Time Domain Reflectometry for Water Content Measurement Using a Composite Dielectric Approach. Water Resources Research 26:2267-2273.

Sabburg, J., J.A.R. Ball, and N.H. Hancock. 1997. Dielectric behavior of moist swelling clay soils at microwave frequencies. IEEE Transactions on Geoscience and Remote Sensing 35:784-787.

SAS Institute Inc. 2000-2004. SAS 9.1 Software. SAS Institute Inc, Cary, NC.

Schoeneberger, P.J., Wysocki, D. A., Benham, E. C., and Broderson, W. D. (editors). 2002. Field book for describing and sampling soils, Version 2.0. 2.0 ed. Natural Resources Conservation Service, National Soil Survey Center, Lincoln, NE.

Topp, G.C., J.L. Davis, and A.P. Annan. 1980. Electromagnetic determination of soil water content: measurements in coaxial transmission lines. Water Resources Research 16:574-582.

USDA-NRCS. 2006. Web Soil Survey [Online] (verified September 4, 2006).

Vogeler, I. 2001. Copper and Calcium Transport through an Unsaturated Soil Column. Journal of Environmental Quality 30:927-933.

Whalley, W.R., R.E. Cope, C.J. Nicholl, and A.P. Whitmore. 2004. In-field calibration of a dielectric soil moisture meter designed for use in an access tube. Soil Use and Management 20:203-206.

Table 2.1
Mean, standard deviation, and range (minimum and maximum) values for physical and chemical characteristics of 383 soil samples used for calibrating TDR moisture measurements.

		All data n = 382			Sinkhole #1 n = 253			Sinkhole #5 n = 129		
Parameter	Units	Mean	Std Dev	Range	Mean	Std Dev	Range	Mean	Std Dev	Range
TDR Moisture	vol. %	21.68	7.46	0.00, 36.10	20.80	7.27	0.00, 35.90	23.41	7.55	6.50, 36.10
Field Moisture	vol. %	40.53	10.72	14.31, 68.62	41.96	11.06	18.38, 68.62	37.70	9.42	14.31, 55.01
Depth	feet	-11.38	6.63	-28.25, -1.25	-12.48	7.00	-28.25, -1.25	-9.20	5.23	-21.25, -1.25
Bulk Density	g/cm^3	1.42	0.27	0.76, 2.54	1.51	0.26	0.89, 2.54	1.25	0.19	0.76, 1.88
Clay	% bulk sample	34.5	12.7	8.6, 67.8	33.3	11.8	13.1, 59.0	36. 9	14.2	8.6, 67.8
Silt	% bulk sample	33.3	11.3	8.7, 71.0	30.5	11.6	8.7, 62.0	39.0	8.2	19.6, 71.0
Sand	% bulk sample	29.5	12.4	6.3, 66.0	33.9	11.8	9.2, 66.0	21.0	8. 5	6.3, 46.0
Gravel	% bulk sample	2.6	4.6	0.0, 30.0	2.4	4.7	0.0, 30.0	3.1	4.4	0.0, 23.0
pH	pH	4.93	0.41	4.20, 6.59	4.81	0.37	4.20, 6.44	5.17	0.39	4.39, 6.59
BpH	BpH	5.98	0.24	5.29, 6.61	5.93	0.25	5.35, 6.61	6.07	0.21	5.29, 6.49
Est CEC	meq/100g	4.52	1.34	0.90, 8.50	4.15	1.18	0.90, 7.70	5.25	1.36	2.00, 8.50
log % Ca Sat	%	1.23	0.35	0.54, 1.88	1.12	0.34	0.54, 1.88	1.47	0.23	0.69, 1.85
log % Mg Sat	%	1.17	0.30	0.38, 1.68	1.06	0.28	0.38, 1.67	1.40	0.18	0.91, 1.68
log % K Sat	%	0.41	0.20	-0.50, 0.88	0.35	0.02	-0.05, 0.86	0.51	0.14	0.11, 0.88
log K	(mg/kg)	1.64	0.19	1.20, 2.08	1.55	0.16	1.20, 2.03	1.81	0.10	1.46, 2.08
log Ca	(mg/kg)	2.17	0.37	1.36, 3.01	2.02	0.34	1.36, 3.01	2.47	0.24	1.73, 3.01
log Mg	(mg/kg)	1.89	0.34	0.85, 2.58	1.74	0.28	0.85, 2.32	2.19	0.24	1.49, 2.58
log Zn	(mg/kg)	-0.23	0.46	-1.00, 2.00	-0.38	0.27	-1.00, 1.39	0.064	0.59	-0.70, 2.00
log Mn	(mg/kg)	0.86	0.60	-1.00, 2.32	0.69	0.58	-1.00, 1.98	1.20	0.46	-0.10, 2.32
log Cu	(mg/kg)	-0.45	0.23	-1.00, 0.85	-0.42	0.22	-1.00, 0.85	-0.51	0.24	-1.00, -0.05
log Fe	(mg/kg)	1.22	0.19	0.72, 1.69	1.25	0.21	0.72, 1.69	1.16	0.15	0.91, 1.51
OM	% bulk sample	1.24	0.44	0.40, 2.80	1.15	0.41	0.40, 2.30	1.41	0.43	0.50, 2.80
Phosphorus	(mg/kg)	4.33	12.49	2.00, 185.00	3.44	11.65	2.00, 185.00	6.08	13.89	2.00, 118.00
Boron	(mg/kg)	0.11	0.025	0.10, 0.20	0.10	0.017	0.10, 0.20	0.11	0.034	0.10, 0.20
Acidity	%	55.59	26.25	0.00, 92.70	65.20	25.12	0.00, 92.70	36.66	16.27	0.40, 77.40
Soluble Salts	ppm	45.03	25.23	1.00, 179.00	36.20	18.65	1.00, 115.00	62.40	27.43	26.00, 179.00

Table 2.2
Final regression statistics for each data set. Top table shows statistics when all data are included in a single model. Bottom tables show statistics resulting from division of data by sinkhole. Correlation coefficients, p-values and measurement errors for each parameter are listed. SD = standard deviation of residuals [% moisture]. One standard deviation in % moisture for weighted error propagation are also shown. Errors shown are either estimated or obtained from published sources (Dane, 2002; IMKO, 2006b)

All Data						
Variable	Coefficient	p-value	Error %	Source for error value		
Intercept	0.053	0.9862			n	382
TDR Moisture	-0.062	0.1919	2	IMKO report	R^2	0.80
Clay	0.881	<0.0001	0.5	Dane and Topp	SD of residuals	4.83
Depth	-0.609	<0.0001	0.35	Estimated	Weighted error	1.70
Silt	0.442	<0.0001	1	Dane and Topp		
Bulk Density	8.542	<0.0001	5	Estimated		
Est CEC	-2.988	<0.0001	10	Estimated		
Log Ca Sat	-7.210	<0.0001	10	Estimated		
Sinkhole #1						
Variable	Coefficient	p-value	Error %	Source for error value		
Intercept	0.921	0.8196			n	253
TDR Moisture	-0.102	0.1240	2	IMKO report	R^2	0.80
Clay	0.917	<0.0001	0.5	Dane and Topp	SD of residuals	4.95
Depth	-0.621	<0.0001	0.35	Estimated	Weighted error	1.34
Silt	0.439	<0.0001	1	Dane and Topp		
Bulk Density	5.206	0.0025	5	Estimated		
Est CEC	-2.806	<0.0001	10	Estimated		
Log Ca Sat	-4.282	<0.0001	10	Estimated		
Sinkhole #5						
Variable	Coefficient	p-value	Error %	Source for error value		
Intercept	7.879	0.1042			n	129
TDR Moisture	0.045	0.4140	2	IMKO report	R^2	0.88
Clay	0.627	<0.0001	0.5	Dane and Topp	SD of residuals	3.40
Depth	-0.508	<0.0001	0.35	Estimated	Weighted error	2.40
Silt	0.291	<0.0001	1	Dane and Topp		
Bulk Density	14.235	<0.0001	5	Estimated		
Est CEC	-1.347	<0.0001	10	Estimated		
Log Ca Sat	-14.361	<0.0001	10	Estimated		

Table 2.3
Parameter estimates, standard error, and t-statistics for categorical variables in the categorical regression model.

Variable and Category	Parameter Estimate	Standard Error	t Value	Pr > | t |
Intercept	27.399	2.158	12.7	<0.0001
TDR Moisture	0.214	0.052	4.11	<0.0001
Depth (<5 feet)	0.000			
Depth (5 to <10 feet)	2.621	0.933	2.81	0.0052
Depth (10 to <15 feet)	3.961	0.978	4.05	<0.0001
Depth (15 to <20 feet)	7.732	1.026	7.54	<0.0001
Depth (20 to <25 feet)	11.205	1.190	9.42	<0.0001
Depth (≥25 feet)	15.061	2.761	5.45	<0.0001
% Clay (<15)	0.000			
% Clay (15 to <30)	5.302	1.546	3.43	0.0007
% Clay (30 to <45)	11.598	1.561	7.43	<0.0001
% Clay (≥45)	13.447	1.756	7.66	<0.0001
% Sand (<20)	0.000			
% Sand (20 to <40)	-4.713	0.844	-5.59	<0.0001
% Sand (≥40)	-9.109	1.159	-7.86	<0.0001
Bulk Density (<1.25) g cm^{-3}	0.000			
Bulk Density (1.25 to <1.75) g cm^{-3}	3.473	0.746	4.66	<0.0001
Bulk Density (≥1.75) g cm^{-3}	5.399	1.200	4.50	<0.0001
Log % Ca Sat. (<1)	0.000			
Log % Ca Sat. (1 to <1.5)	-3.117	0.733	-4.25	<0.0001
Log % Ca Sat. (≥1.5)	-7.030	0.827	-8.50	<0.0001
Est CEC [meq/100g] (<3)	0.000			
Est CEC [meq/100g] (3 to <5)	-2.346	0.996	-2.36	0.0191
Est CEC [meq/100g] (5 to <6)	-6.206	1.164	-5.33	<0.0001
Est CEC [meq/100g] (≥6)	-7.294	1.353	-5.39	<0.0001
% Organic Matter (<1)	0.000			
% Organic Matter (1 to <1.5)	4.101	0.917	4.47	<0.0001
% Organic Matter (≥1.5)	5.040	1.120	4.50	<0.0001

CHAPTER 3

Linking Field Scale Electrical Resistivity Tomography and Time Domain Reflectometry Derived Soil Moisture

Benjamin F. Schwartz[1], Madeline E. Schreiber[1] and Tingting Yan[2]
[1]Department of Geosciences
Virginia Polytechnic and State University
Blacksburg, VA 24060
[2]Intera, Inc., Austin, TX 78754

ABSTRACT

Electrical Resistivity Tomography (ERT) and Time Domain Reflectometry (TDR) were used to simultaneously measure resistivity and soil moisture at an experimental field site with the objective of developing a non-invasive method for measuring 2-D soil moisture profiles in unsaturated zones. Using the field data, we developed a model using a modified form of Archie's Law, which uses bulk conductivity derived from ERT readings, pore water conductivity, and percent clay content of soils, to convert 2-D ERT profiles into 2-D soil moisture profiles. We numerically optimized and calibrated the model using 1-D access-tube Time Domain Reflectometry (TDR) derived soil moisture measurements. Results show that the model can be successfully applied to highly heterogeneous soils, and thus provides a useful tool for measuring 2-D soil moisture at a variety of field sites.

INTRODUCTION

Measuring and modeling soil moisture in unsaturated environments is difficult due to the complexity of unsaturated hydrogeologic systems and difficulties associated with obtaining accurate and spatially representative measurements of soil moisture in a heterogeneous environment. Tools commonly used for measuring soil moisture include Time Domain Reflectometry (TDR) and neutron probes. However, the challenge in using these tools is that previous work has shown that TDR and neutron methods produce measurements of soil moisture that can be inaccurate without material specific calibrations for many soil textures (Dane, 2002; Jacobsen and Schjonning, 1993; Schwartz et al., *In review;* Yao et al., 2004).

Theoretical, field, and lab-based studies have documented that relationships exist between various physical properties in the unsaturated zone (such as moisture content) and geophysical measurements (Auerswald et al., 2001; Kalinski and Kelly, 1993; Kalinski et al., 1993; Maulem

and Friedman, 1991; Titov et al., 2004). The advantage of using geophysical tools such as electrical resistivity tomography (ERT) or ground penetrating radar (GPR) is that they provide a non-invasive method for measuring or inferring soil characteristics, such as soil moisture. A limitation of many of these studies is that they often rely on a single geophysical technique to quantify soil properties, and thus lack methods for verification or validation.

Laboratory studies correlating geophysical measurements and soil properties (e. g., soil resistivity *vs.* soil moisture) are by nature conducted at small scales. Thus, a limitation of these studies is that the strong correlation observed between electrical and physical parameters is often related to the scale of measurement and the level of control over the experiment. In general, lab-scale soil resistivity *vs.* soil moisture experiments generate results which are not reproducible in the field due to problems such as heterogeneities in large-scale natural systems and decreasing resolution of geophysical measurements with depth. As an example, Kalinski and Kelly (1993) were able to show excellent correlation between measured soil electrical resistivity and volumetric soil moisture at the centimeter scale. Achieving similar results using field-scale measurements would not be possible because of lower resolution at larger scales and uncertainties related to poorly characterized heterogeneities in physical and chemical properties which influence electrical properties.

In the field, geophysical techniques have been used to non-invasively characterize unsaturated soil hydrology with varying degrees of success (Kalinski and Kelly, 1993; Lambot et al., 2004; Michot et al., 2003; Zhou et al., 2001). In contrast with lab-scale studies, field-scale geophysical studies of unsaturated soils are frequently qualitative rather than quantitative. For example, one promising method for inferring soil moisture in the field is electrical resistivity tomography (ERT), which has been used in a variety of geologic settings to study temporal variability in soil moisture (Barker and Moore, 1998; Daily and Ramirez, 2000; Hauck and Scheuermann, 2005). Use of ERT to measure temporal variations in soil moisture assumes that changes in soil resistivity result from some change of unknown magnitude in soil moisture, and that wetting or drying soils will result in decreasing or increasing resistivity values, respectively. Although ERT is a very useful tool, there are several limitations to using ERT as a stand-alone method for measuring soil moisture. For example, simply converting raw resistivity data into soil moisture values is next to impossible without a more detailed understanding of the physical and chemical properties of the subsurface. Likewise, developing a resistivity *vs.* soil moisture calibration

curve on an in-situ sample is hindered by the difficulties associated with accurately and simultaneously measuring both of these parameters in the subsurface.

There are additional challenges to conducting field-scale studies using geophysical methods to estimate soil moisture. First, there are practical issues such as variable resolution of non-intrusive measurement techniques (e.g., GPR and ERT), penetration depth being dependent on physical conditions (e.g., high clay content limits the effective depth of penetration for GPR), and the physical difficulty and cost associated with directly measuring hydrogeologic parameters in unsaturated environments. Integrative approaches which combine geophysical modeling and hydrogeologic data yield better results (Shuyun and Yeh, 2004). Results of this type of approach emphasize the value of incorporating hydrogeologic data in geophysical models.

Spatial and temporal distribution of soil moisture also needs to be addressed. In the field, relatively small-scale direct measurements of soil moisture and physical properties are the only scale at which these parameters may be collected in-situ, especially if the system being studied is not destroyed in the process of collecting the information. This means that interpolation, extrapolation, and other methods of modeling these properties (e.g., geophysical techniques) are the only alternatives for obtaining larger-scale coverage for the parameters of interest. For example, TDR measurements can provide an estimate of soil moisture within a region extending only tens of centimeters of the probe - a definite limitation in situations where the region of interest is actually tens of meters. Conversely, techniques such as ERT provide geophysical evidence of physical properties in the subsurface at many different scales and resolutions. However, directly interpreting the ERT results in terms of a parameter such as soil moisture becomes extremely difficult without additional information. This is where linking two or more data sets such as large scale ERT measurements, and small scale soil moisture measurements and physical properties can be useful.

The primary objective of this study was to develop a method for converting field-scale 2-D ERT profiles into 2-D soil moisture profiles. We approached this research problem by investigating links between small-volume (cm-scale) moisture measurements from access-tube Time Domain Reflectometry (TDR), and large volume (meter-scale) electrical measurements made using 2-D Electrical Resistivity Tomography (ERT). Developing methods for linking ERT and TDR would be useful for unsaturated zone characterization as ERT gives 2-D coverage of a study area and

can model variations in subsurface properties which may not be detected using 1-D methods such as TDR. In addition, if 2-D ERT can be used to estimate soil moisture in heterogeneous soils, it would provide an excellent tool for non-invasive characterization of almost any unsaturated soil system.

FIELD SITE

Our research site at the Virginia Tech Kentland Experimental Farms in Montgomery County, Virginia contains two well-developed sinkhole plains formed in ancient New River terraces **(Figure 3.1a)**. The sinkholes are generally broad and shallow, allowing easy access for agricultural activities, and contain no bedrock outcrops. Thick terrace deposits mantle sinkholes with soils characterized as weathered fluvial terrace materials deposited by the ancient New River, which have developed over the underlying Cambrian aged Elbrook Formation limestone and dolostone bedrocks. Soils are classified by the USDA-NRCS as Guernsey silt loam, Unison and Braddock soils, and Unison and Braddock cobbly soils (USDA-NRCS, 2006). Both sinkhole plains have numerous sinkholes of similar size and shape. Two sinkholes were chosen for more detailed analysis in our study. Sinkhole #1 is in a higher and older terrace deposit and contains highly weathered soils to depths exceeding 40 feet (12.2 m). Sinkhole #5 is formed in a lower and younger terrace and contains soils which are not as mature. In Sinkhole #5, bedrock was reached in most augered holes at depths between 11 and 25 feet (3.4 and 7.6m) below land surface.

METHODS

Sinkhole characterization

We characterized the physical and chemical properties of the sinkholes by collecting and analyzing soil samples at 12-inch (30.5 cm) intervals during access tube installation. Samples were also collected at larger intervals during installation of deeper monitoring wells (10 to 12m). Except for one monitoring well in sinkhole #1, water levels were not detected in any of the wells. A well in sinkhole #1 had <1m of water in it for a short time after installation, which was more than a year before the ERT and TDR measurements used in this study were collected. The absence of water in the monitoring wells since then is likely the result of considerably drier conditions since the wells were installed and is evidence that saturated conditions were remained well below the bottom of all TDR access tubes. Detailed topographic surveys performed in each

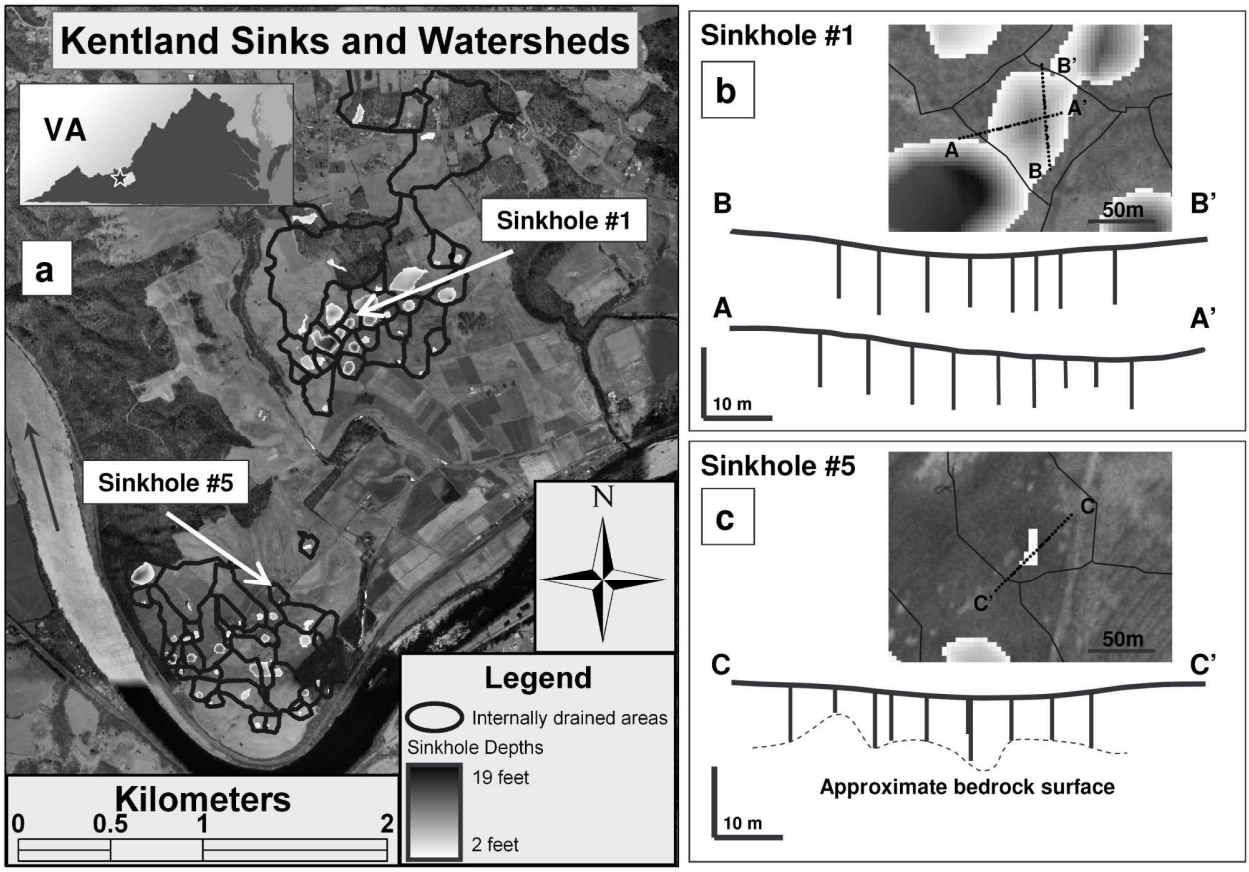

Figure 3.1 Field site and ERT transect locations

a) Virginia Tech Kentland Experimental Farms at Whitethorne, Virginia, USA. **Figure 3.1a** shows study sinkholes #1 and #5 and catchment areas (adjacent polygons) for each sinkhole within the two sinkhole plains. Aerial imagery © 2002 Commonwealth of Virginia. Sinkhole #1 is in the higher, older terrace. b) and c) show surface topography and the location and orientation of instrumentation installed in transects across both sinkholes. Upper image in the diagrams is a map view of the sinkhole, while the lower portion of the diagrams shows profile views of monitoring wells, TDR access-tubes and other instrumentation installed along each transect. Note that depth of bedrock was not determined in Sinkhole #1.

sinkhole include elevations and locations of all monitoring wells, access tubes, and ERT electrodes.

Soil Analyses

Soil moisture was determined gravimetrically for each soil sample by drying in an oven at 105°C until repeated weighing showed no further weight loss. Percent soil moisture by volume and dry bulk density were calculated using final oven-dry weight, initial weight and the sample volume. Particle size analyses (PSAs) were performed on each sample using the ASTM 152H hydrometer method described in Dane (2002) to measure percent clay. Percent sand was then measured by thoroughly washing each sample through a 53 μm sieve and drying the retained sand at 105°C. The dried sediments were shaken on the sieve to remove any remaining silt or clay. The sand fraction was then weighed and recorded. Percent silt was calculated by difference from the initial 40.0 g sample of $\leq$2.0 mm material. A split of each sample was analyzed for standard soil chemical parameters, including pH, BpH (buffer pH, a measure of a soil's natural buffering capacity), acidity, base saturation, Ca saturation, Mg saturation, K saturation, estimated Cation Exchange Capacity (CEC), total soluble salts (TSS), organic matter (by loss on ignition), and the following Mehlich 1 extractable nutrients: P, K, Ca, Mg, Zn, Mn, Cu, Fe, and B. Analyses were performed by the Virginia Tech Soil Testing and Plant Analysis Laboratory using the methods described by Mullins (2005).

Time Domain Reflectometry

We used a TRIME T3-50 IPH Tube Access Probe TDR unit (manufactured by IMKO of Germany) connected to a laptop computer in the field to measure and record uncalibrated percent moisture by volume. The TRIME T3-50 IPH probe is specially designed for use in PVC access-tubes which allow vertical moisture profiles to be measured by lowering the instrument inside tubes to the desired depths. We installed a total of 23 access tubes (made of Schedule 40, 2.375-inch (6.03 cm) outer diameter PVC) in two transects across sinkhole #1 and one transect across sinkhole #5. Each access-tube consists of standard threaded and o-ring-sealed-joint PVC well-casing sealed at the bottom with a glued PVC well-point.

TDR measurements for this study were collected at six-inch (15.2 cm) depth intervals in each access tube and then adjusted to represent calibrated field moisture values using calibration equations which were developed using select physical and chemical parameters of the soils (see

(Schwartz et al., *In review*)). The calibration was required because our TDR moisture measurements significantly and consistently underestimated soil moisture. Briefly, we used a multiple linear regression model to calibrate the TDR measurements to gravimetrically measured moisture content. In addition to TDR moisture, the model includes effects of the following physical and chemical parameters which were obtained from the soil sample analyses: percent clay, depth, percent silt, bulk density, cation exchange capacity, and log of percent calcium saturation.

Electrical Resistivity Tomography

ERT data for this study were collected by measuring three 2-D dipole-dipole ERT profiles on May 17, 2006 (1-D access-tube TDR soil moisture profiles were also measured on the same day in all of the access-tubes). The dipole-dipole array was chosen because of its reported sensitivity to the soil- bedrock interface (Zhou et al., 2000). Prior to measurements, three permanent arrays of 25 carbon electrodes each were installed in transects across the study sinkholes using 3m electrode spacing. The transects lie directly over and along the TDR access-tube transects (**Figure 3.1 b, and c**). Electrodes are 12 inches (30.5 cm) in length and are electrically coupled to the surrounding soils using alternating compacted layers of bentonite clay and native soil in a 13 inch (33 cm) augered hole. Electrodes were protected from disturbance by farming activities by installing the electrodes slightly below the ground surface and covering them with a removable PVC cap. A Campus Geopulse DC electrical resistivity meter with a 240m long, 25 take-out cable was used to measure ERT profiles. ERT data were processed using the EarthImager 2D software package from Advanced Geosciences, Inc (Advanced Geosciences, 2005). The software converts measured apparent resistivity values into a modeled distribution of subsurface resistivity values through the use of an iterative resistivity inversion model.

LINKING ERT AND TDR DERIVED SOIL MOISTURE

Archie's Law

Examination of ERT measurements vs. TDR-derived soil moisture (**Figure 3.2**) reveals that there is no clear simple relationship between them. Potential difficulties in finding a relationship include different ERT-moisture relationships for soils with different physical or chemical properties, and issues related to both the scale of ERT vs. TDR measurements and the decreasing resolution of ERT with depth. As examples: percent clay will significantly affect both electrical properties and moisture content of soils; and the scale of TDR-measurement is 15 cm or less

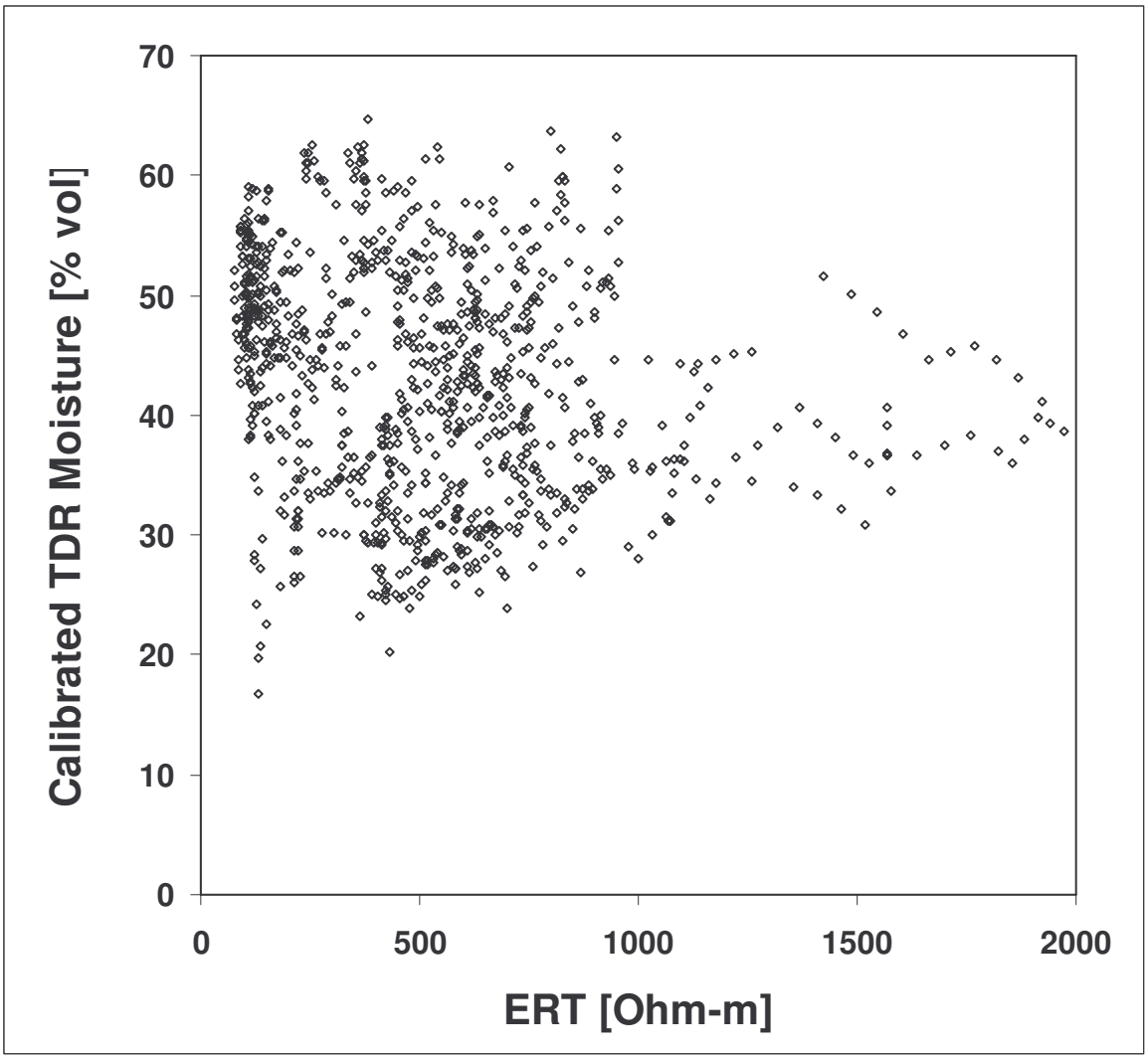

Figure 3.2 Plot of uncalibrated ERT vs. calibrated TDR moisture
Plot illustrating the original relationship between our calibrated TDR soil moisture values and modeled ERT data.

from the probe while ERT is modeling electrical properties at a much larger scale. To investigate a possible relationship between ERT and TDR-derived soil moisture, we utilized a numerically optimized and modified form of Archie's Law to derive soil moisture from ERT measurements. Archie's Law was originally developed and used to link borehole resistivity logs with porosity of surrounding petroleum reservoir rocks (Archie, 2003). Since then, variations of this relationship have been developed which also explain the relationship between electrical properties of a material and certain physical properties, such as porosity of saturated materials or moisture content in unsaturated soils. As an example, a modified form of Archie's Law has been developed by Shah and Singh (2005) to describe the relationship between electrical resistivity and soil moisture:

$$\sigma_b = c \cdot \sigma_w \cdot \theta^m \quad \textbf{(1)}$$

Where σ_b is bulk conductivity, σ_w is pore water conductivity, θ is moisture content, and c and m are fitting parameters that depend primarily on the particle size characteristics of the soil. Shah and Singh (2005) also proposed the following empirical relationships between c and m, and the clay content of a soil.

$$c = 0.6 \cdot Clay^{0.55} \quad \textbf{(2)}$$

$$m = 0.92 \cdot Clay^{0.2} \quad \textbf{(3)}$$

Where clay is expressed as percent by volume and is $\geq$ 5%. For clay contents of less than 5% these parameters become constants: c = 1.45 and m = 1.25. Shah and Singh (2005) relate fitting factors c and m to volumetric soil moisture through: $\sigma_b/\sigma_w = 1/F = c \cdot \theta^m$, where F is a formation factor.

We rearranged terms in **(1)** to solve for θ, which results in:

$$\theta = \left(\sigma_b / c \cdot \sigma_w\right)^{1/m} \quad \textbf{(4)}$$

Further refinement of the modified Archie's Law

To use **(4),** which would allow us to relate ERT values to the 1-D TDR-derived soil moisture measurements [θ_{TDR}] from our field site, we needed to measure or estimate σ_w, σ_b, *c*, *m*, and clay. We obtained estimated values of σ_b from the inverse of our modeled ERT values [σ_b = 1/ ERT] for the locations which correspond to θ_{TDR} measurements. Because our θ_{TDR} data are obtained from 1-D profiles, we extracted 1-D ERT data from 2-D ERT profiles which correspond to the θ_{TDR} measurement locations. Linear interpolation was then used to generate 1-D ERT data at the

same data intervals as our θ_{TDR} measurements, which are at six inch (15.2 cm) depth intervals. Clay contents for these locations were measured (as described above in Chapter 2) in 470 soil samples collected during TDR access-tube installation.

Issues related to comparing moisture measurements at different scales are difficult to address. TDR measurements represent small-volume measurements (not more than 15 cm from the probe), while ERT measurements were made using 3 m electrode spacings with a dipole-dipole array. Because of the difference in scale, the ERT-derived moisture measurements represent a 'smoother' model of the subsurface and do not accurately represent small-scale heterogeneities. Conversely, TDR is very sensitive to small-scale heterogeneities and may, in many cases, be over-emphasizing small-scale heterogeneities which have little effect on bulk soil moisture: particularly those related to small voids of cobbles. Reducing the electrode spacing for ERT arrays would have increased the resolution of the model and its sensitivity to small-scale heterogeneities without significantly changing the bulk characteristics of the model. However, because we installed permanent electrode arrays, modifying the spacing was not practical after the experiments began. In future work we would reduce the electrode spacing to obtain a higher resolution over the depth of physical characterization - perhaps 10 to 12 m rather than 15 to 20 m. While this research does not investigate the physical or theoretical limitations of comparing these two types of measurements at two different scales, it does show that a reasonable model can be obtained by using data which represent two different scales of measurement.

Accurately measuring σ_w is very difficult, even using direct measurement methods such as extraction of pore water or soil-paste electrical conductivity methods (Rhoades et al., 1989). The soil-paste method relates the electrical conductivity of a saturated soil paste to the extracted pore-water conductivity. Because we were unable to extract and measure pore water conductivity directly on our samples, and the soil paste method was deemed too time intensive for use on each sample, we estimated σ_w using the two different methods described below.

Soluble salts as a proxy for σ_w

The first method we used for estimating σ_w involved converting the soluble salts (SS) measurements from the soil analyses into electrical conductivity values. The original lab measurement used to calculate SS values is an electrical conductivity measurement [siemens x 10^{-5}] of a 1:2 (vol/vol) soil-water mixture (Mullins, 2005). SS is then converted into ppm in a

1:1 solution by multiplying EC by 6.4 x 2. The conversion factor from siemens to ppm is 6.4 and 2 is the dilution factor. This method assumes a KCl standard. By reversing this calculation, and then converting siemens x 10^{-5} to units of S/m, we can approximate the pore water conductivity. Obviously, the true pore water conductivity in the field would have differed from this estimate since the original soil moisture content was not a consistent 50 percent by volume in all samples. We also recognize that pore water conductivity values change over time and will not remain identical to what they were at the time our soil sample were collected. However, we believe it is reasonable to assume relatively small changes (especially at greater depths) for most samples.

One limitation we encountered with this proxy is that the SS values for our soils are so low that many of the original conductivity measurements on 1:2 soil-water mixtures were at or below the detection limit of the conductivity meter and were therefore simply reported as being the lowest measurable conductivity value. This means that samples with low pore water conductivity are assigned an SS value that over-predicts conductivity, which influences later calculations of σ_w.

Extractable Cations as a proxy for σ_w

Because the soluble salts proxy was complicated by low detection limits, we used a second proxy for pore water conductivity which assumes there is some relationship between certain extractable cations and equilibrium or near-equilibrium pore water conductivity in a soil sample. Each of the soil samples collected during TDR access-tube installation were subjected to a soil chemical analysis, which includes measurement of Mehlich 1 extractable cations (P, K, Ca, Mg, Zn, Mn, Cu, Fe, B) (Mullins, 2005). Extractable basic cations in our soil samples are dominated by Ca and Mg (~80%) so we chose to use these cations based on the assumption that they will also control pore water conductivity. The sum of Ca and Mg (reported in the soil analyses as ppm in soil, or mg/kg) was divided by 640 to convert from ppm to conductivity in the extracted solution, and then by 10 to reduce the number to an order of magnitude that would be more representative of actual pore-water conductivity values. If a relationship does exist between extractable cations and σ_w, this value can reasonably be assumed to be a proxy for σ_w.

Further justification for the use of extractable cations was found in the relationship between cations, depth, and clay mineralogy (which strongly influences cation exchange capacity (CEC) of clay-rich soils) at our field site. In additional to the textural heterogeneity at our field site, soils are also heterogeneous in terms of mineralogy for all sediment size fractions. For clay

minerals in particular, Harris et al (1980) reported that a site in the upper terrace (assumed to be equivalent to sinkhole #1) contained clays which were dominated by kaolinite, hydroxy interlayered vermiculite, and vermiculite, with kaolinite and vermiculite increasing with depth and hydroxy interlayered vermiculite decreasing with depth. The depth of investigation in their study was limited to 2.5 m, so it is unclear what trends might exist below this depth, but one indication that the kaolinite and vermiculite content may remain constant at depths greater than 2.5 m in sinkhole #1 is the fact that extractable Ca and Mg tend to decrease sharply with depth to around 3m before remaining essentially constant with depth below 3m **(Figure 3.3)**. Since hydroxy interlayered vermiculite and vermiculite have a very high CEC compared to kaolinite, we hypothesize that one reason for nearly constant extractable Ca and Mg at depths below 3 m may simply be a nearly constant CEC with depth. A slight decrease in CEC with depth may be only related to slightly decreasing clay content with depth, but with no appreciable changes in the mineralogy-related CEC **(Figure 3.4)**. Without a more detailed investigation of clay mineralogy in our samples, the true relationships between extractable cations, CEC and clay mineralogy at our site is difficult to determine. Significantly higher values of extractable Ca + Mg near the surface are probably related to the application of agricultural lime. Interestingly, the Ca + Mg profile from the access tube installed in the bottom of sinkhole #1 does not show a decreasing trend in Ca + Mg (**Figure 3.3**). An explanation for this could be that rainwater (especially overland flow) is preferentially infiltrating at the bottom of the sinkhole (an observation supported by physical observations during heavy rain events) and has carried these cations downward during infiltration after application of lime at the surface.

Optimizing the parameters for fitting factors c and m

By defining calibrated TDR moisture as the dependent variable, using the derived or measured values of σ_w, σ_b, and percent clay as independent variables, and designating the four coefficients and exponents of c and *m* in **(2)** and (**3)** as unknown parameters, we numerically optimized the equation and solved for the best values of the parameters. Data used for optimization are the extracted 1-D ERT data from locations where both TDR moisture values and soil properties were obtained. The results of the optimization are later used with interpolated values of the independent variables to calculate the 2-D ERT-derived soil moisture profiles. Numerical optimization of **(4)** for the four parameters in **(2)** and (**3)** was performed using a Modified Gauss-Newton iterative numerical model in UCODE 2005, which is a universal inverse modeling program (Poeter et al., 2005). We used UCODE to find the global minima for the model

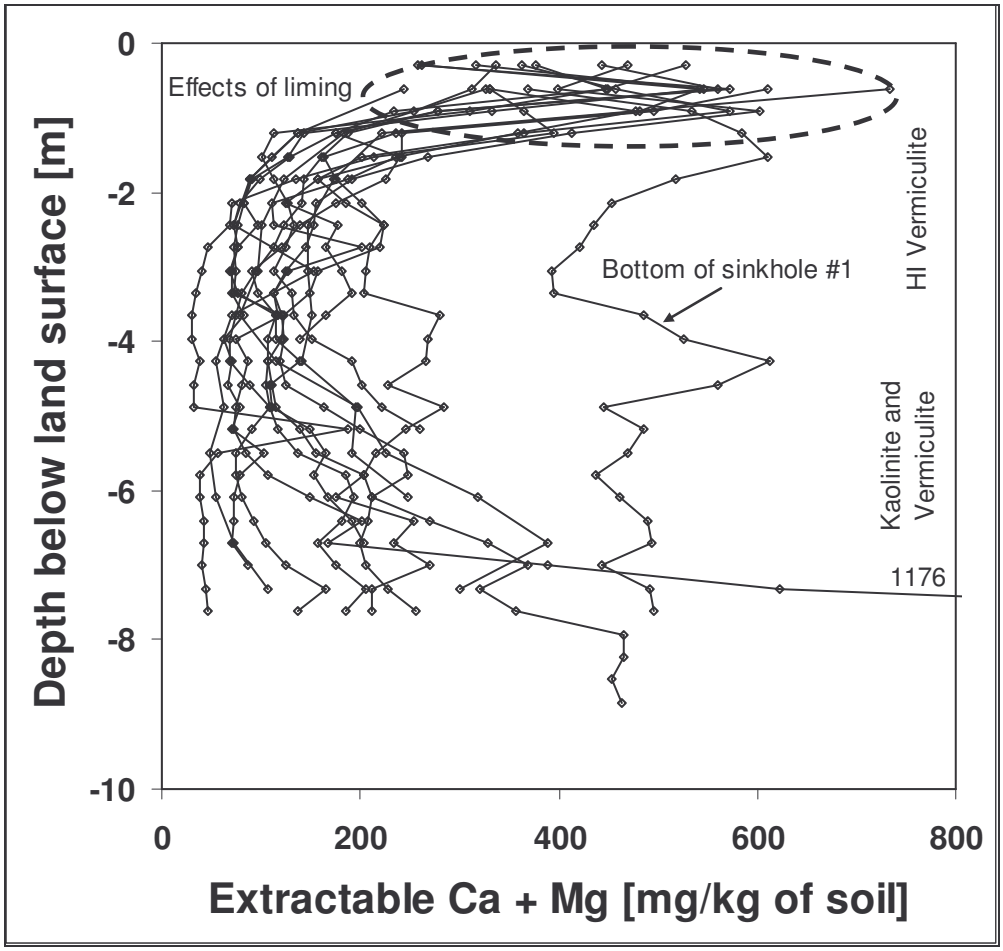

Figure 3.3 Extractable Ca and Mg vs. profile depth
Diagram illustrating the general decrease in extractable Ca and Mg to around 3m in depth for sinkhole #1. Each 1-D profile is from analyses of soil samples collected during access-tube installation in sinkhole #1. 'Bottom of sinkhole #1' indicates the profile from the lowest point in sinkhole #1. One profile had very high extractable Ca and Mg near the bottom and is shown extending off the diagram to a value of 1176 mg/kg. This may indicate the presence of an otherwise undetected carbonate bedrock pinnacle or weathered bedrock instead of fluvial sediments. Based on work by Harris (1980), we have labeled the regions which correspond with depth intervals where hydroxyl interlayered vermiculite, vermiculite and kaolinite likely dominate clay mineralogy. High Ca + Mg near the surface is probably the result of agricultural lime application and not clay mineralogy (area inside dashed oval).

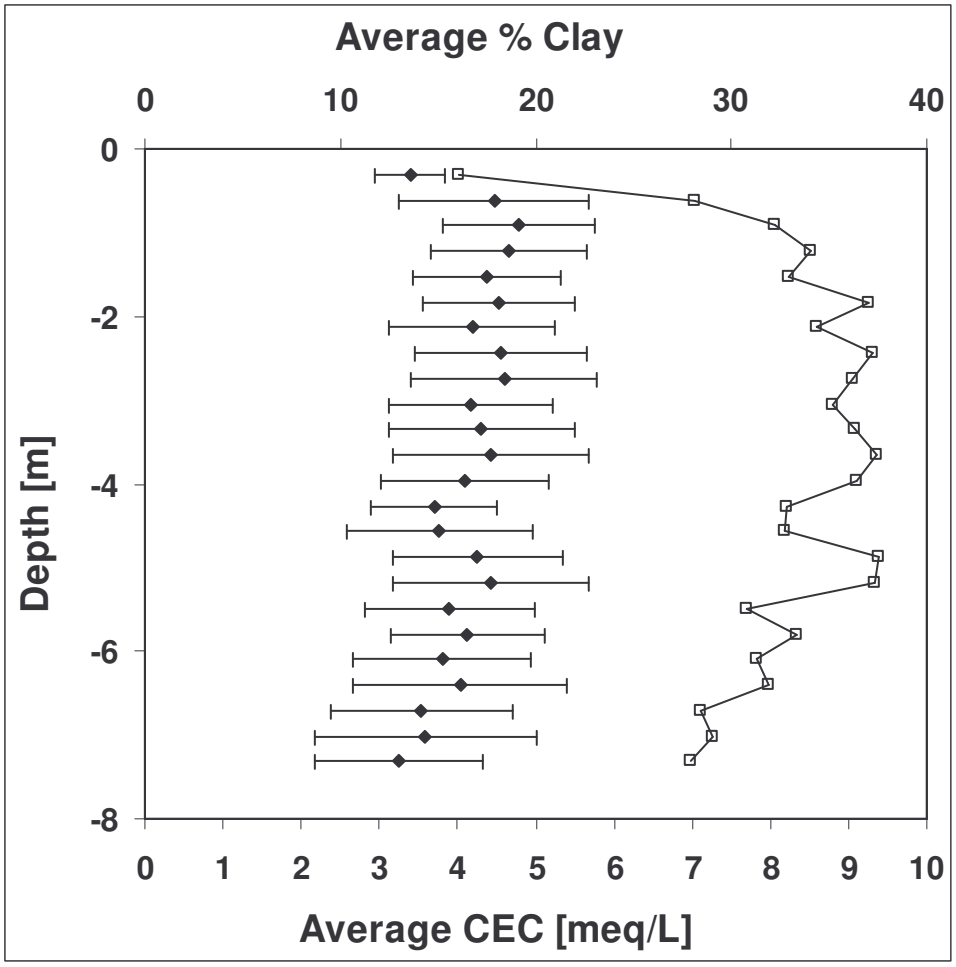

Figure 3.4 Mean CEC and % clay vs. depth
Cation exchange capacity (CEC) averaged by sample depth interval of 0.3048 m (1 ft) in sinkhole #1 (filled diamonds). Note gradual decrease in CEC with depth, is likely related to changes in clay mineralogy, decreasing organic material with depth, and changes in average clay content with depth. Error bars for CEC represent one standard deviation for each averaged depth interval. Average percent clay for the same depth intervals is shown by open squares. Number of samples = 317.

solution. We tested the UCODE's ability to find a global minimum by running the same optimization problems with several different sets of starting values for the four unknown parameters. The model converged on the same solutions regardless of starting values.

Interpolating 1-D data for derivation of 2-D moisture profiles

We used a multi-step process to obtain a final 2-D ERT-derived profile of soil moisture. The first step involves taking the 1-D calibrated TDR moisture, percent clay, and pore-water conductivity data and interpolating between access-tube derived data points using linear kriging with a horizontal to vertical anisotropy ratio of 5:1 and angle settings. By incorporating a horizontal bias in the interpolation process, the results more accurately reflect the sub-horizontal layering in the ancient fluvial sediments which was observed during sampling. Angle settings were used in profile A-A' (**Figure 3.1** and **Figure 3.5)** to more effectively model the consistent dip of soil layers in the profile. Soil layers tend to be sub-horizontal on sinkhole flanks due to draping as the underlying bedrock is removed. After the data are interpolated, 2-D grids of points with 0.5m spacing and identical node locations are produced. The 2-D ERT model is likewise converted to a 0.5m grid of bulk conductivity data using the same node locations, though without including any horizontal bias or angle settings in processing the data. With these identically spaced grids created, we tabulated the data in spreadsheets and used **(4)** to convert bulk conductivity, pore water conductivity, and percent clay into ERT-derived soil moisture values.

RESULTS AND DISCUSSION

Figure 3.5 shows the locations of access tubes with respect to the corresponding ERT profiles for sinkholes #1 and #5. In sinkhole #5 we interpreted a soil-bedrock interface based on information collected during augering and interpretation of ERT data between the access-tubes and monitoring wells. The access tubes shown also represent the locations of 1-D profiles where all soil samples were collected for the physical and chemical characterizations.

Using values we estimated or calculated for σ_w and σ_b, and measured percent clay, we tested the modified form of Archie's Law proposed by Shah and Singh (2005) by calculating soil moisture values using **(4)** with **(2)** and **(3)**, which use their values of model parameters for fitting factors *c* and *m***.** The initial results are shown in **Figure 3.6**. While these results did not show a strong correlation between θ_{TDR} and θ_{calc}, there was clearly a relationship which was not initially present between ERT values *vs.* calibrated TDR soil moisture (**Figure 3.2**)**.** Following numerical

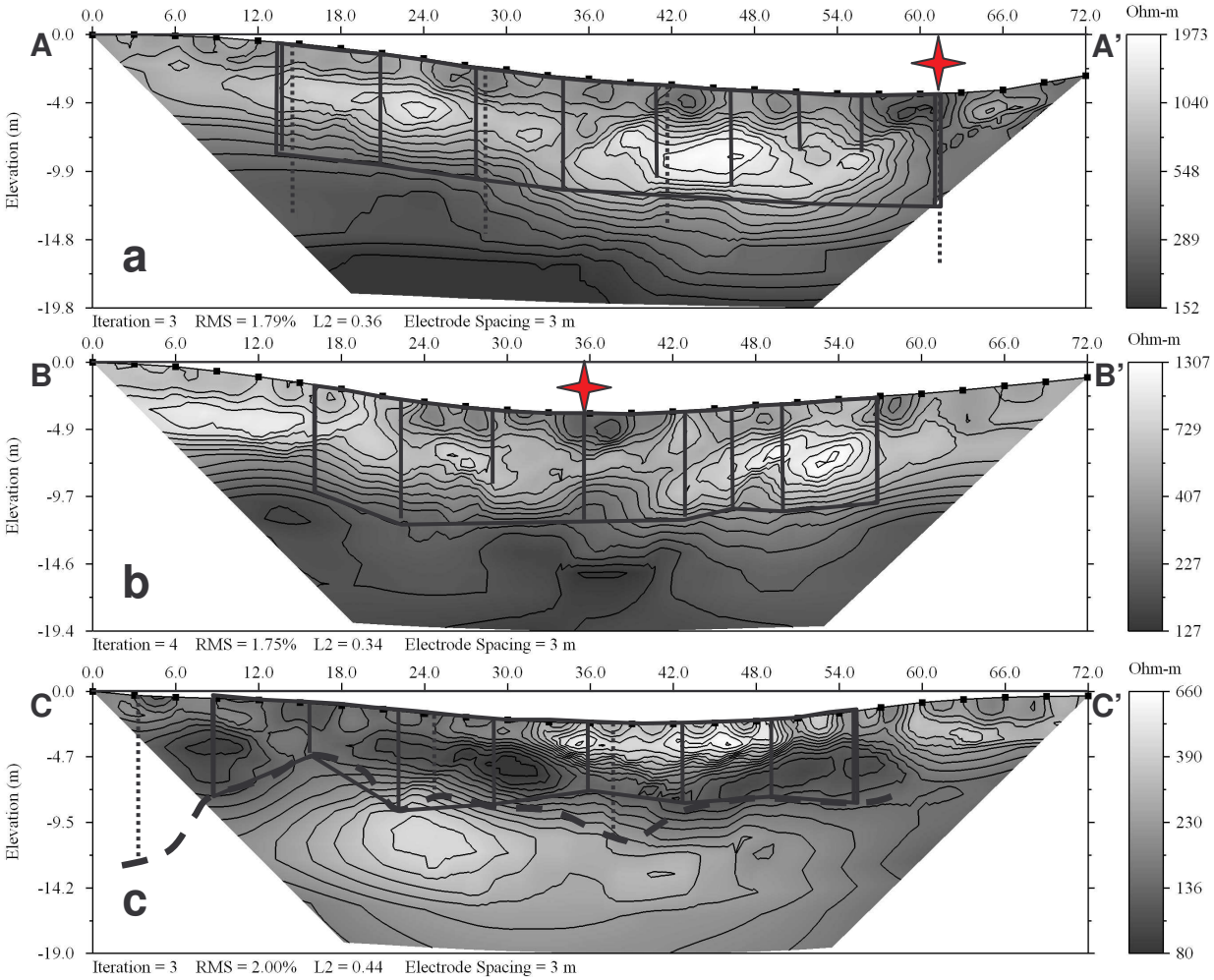

Figure 3.5 ERT profiles

ERT profiles for each transect showing contoured resistivity values, access tubes (solid vertical lines), monitoring wells (dashed vertical lines), bedrock-soil interface (bold dashed line in c)), and outlines of regions where variables were interpolated and kriged to produce profiles. a) and b) show transects across sinkhole #1 while c) is across sinkhole #5. Stars indicate the point where a) and b) intersect. A, A', B, B', C and C' represent transect endpoints as shown in **Figure 3.1**. Also note that the resistivity scales are not the same for each profile

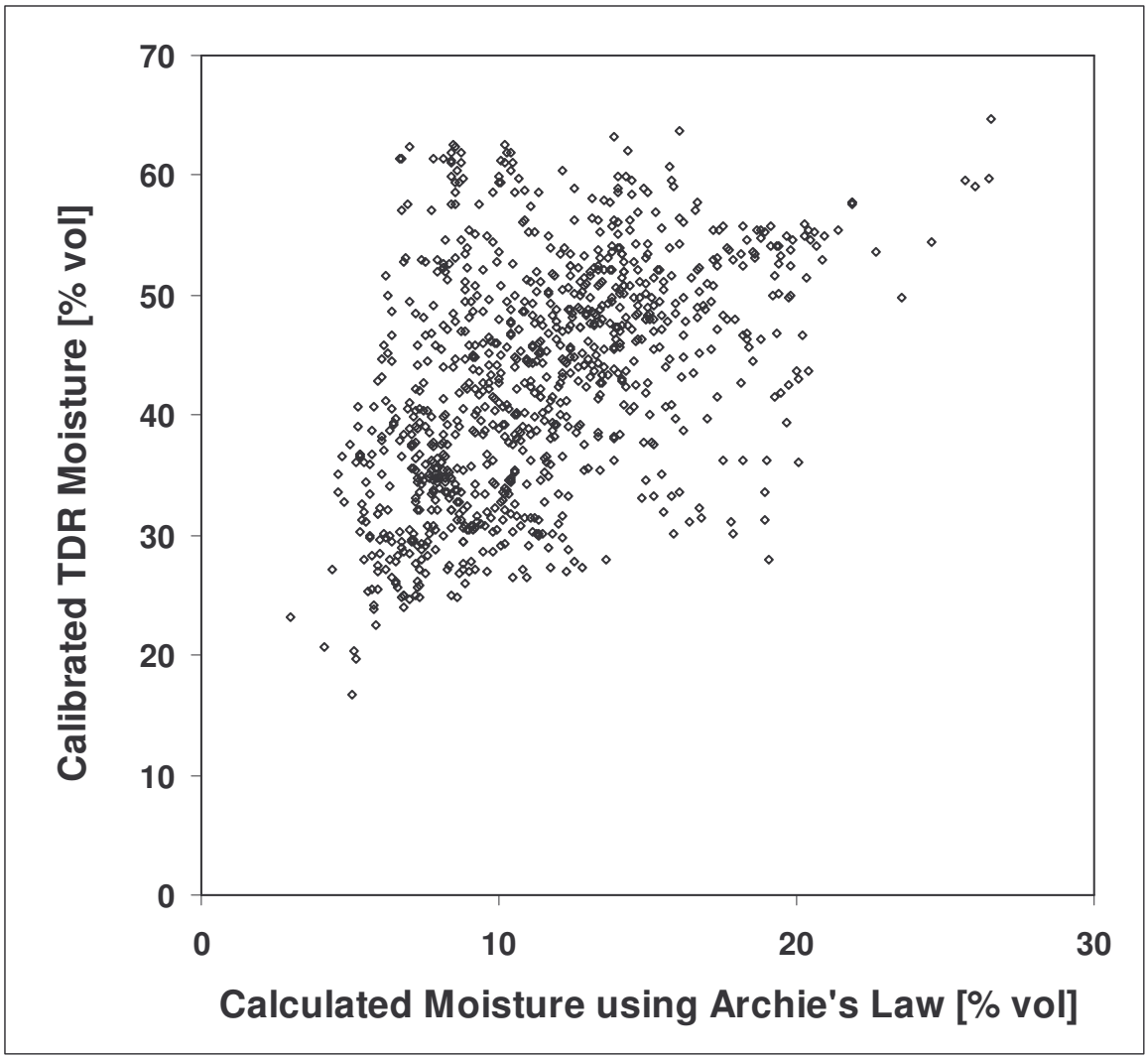

Figure 3.6 ERT moisture vs. TDR moisture
Results of using a modified form of Archie's law as presented by Shah and Singh (2005) using our data with a soluble salts estimate of pore water conductivity.

optimization of the four parameters in **(2)** and **(3)** and using the Ca + Mg proxy for σ_w**,** we derived:

$$c = 0.00873 \cdot Clay^{2.608} \quad \textbf{(5)}$$

$$m = 0.4848 \cdot Clay^{0.8183} \quad \textbf{(6)}$$

Using the numerically optimized fitting factors *c* and *m* in **(4)** gave significantly improved results (**Figure 3.7**) when compared with **Figure 3.6** and **Figure 3.2**. Between the two methods for estimating σ_w, we chose to use the Ca + Mg extractable cation proxy of pore water conductivity in our final calculations rather than the soluble salts estimate because of improved results using the cation proxy (R^2 of 0.57 vs. 0.53). We believe that the soluble salts estimate probably would have produced better results if many of the total soluble salts measurements for our soil samples were not below the instrument resolution in the 1:2 soil-water mixtures.

Shah and Singh (2005) showed that variations in the value of fitting factors *c* and *m* are related to differences in percent clay in the soil. For the fitting factors c and *m,* they reported ranges of 0.33 to 15.85 (for c) and 0.74 to 3.92 (for m). Their calculations were based on measured pore water conductivity data, which we did not have. Using the numerical optimization and our Ca + Mg proxy for σ_w, we derived **(5)** and **(6)** which resulted in fitting factors values ranging from 0.029 to 454.50 (for c) and 0.707 to 14.64 (for m). The values of the four numerically optimized parameters we use for coefficients and exponents of fitting factors *c* and *m* in **(5)** and **(6)** are different than those used by Shah and Singh (2005). We believe these range differences can be explained by the fact that our estimates of pore water conductivity are based on a proxy for σ_w rather than the true values. In the optimization process, adjustments were made to the four parameters (which then changed the fitting factor values) until the best fit between θ_{TDR} and θ_{calc} was achieved. Additionally, the fitting factors are related to the physical and chemical properties of soils and pore waters. If a proxy for the physical property pore water conductivity is used, it follows that the derived fitting factor values may not fall within the same range as those obtained using measured pore water conductivity.

Figure 3.8, Figure 3.9 and **Figure 3.10** show the results of using **(4)** with **(5)** and **(6)** to generate 2-D soil moisture profiles for three sinkhole transects and how the θ_{calc} distribution relates to percent clay, estimated σ_w, and ERT data which were used in calculations to obtain θ_{calc}. **Figure 3.8** and **Figure 3.9** show the modeled and measured distribution of data in sinkhole #1, while

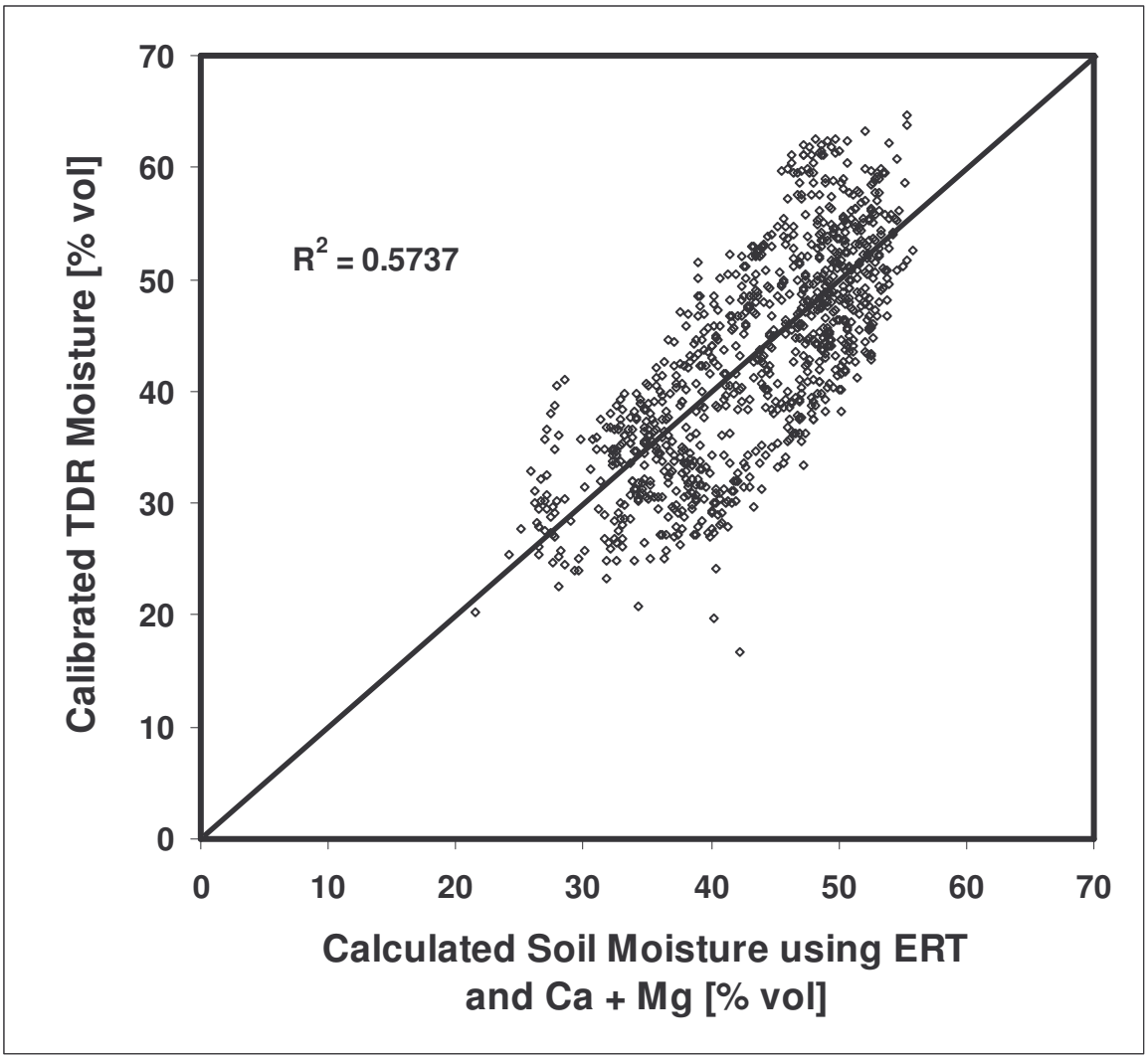

Figure 3.7 Optimized ERT moisture vs. TDR moisture
Plot showing results of using the modified form of Archie's Law to calculate soil moisture from ERT data after numerical optimization**.** These results were obtained using a Mehlich 1 extractable cation proxy (of Ca and Mg) for pore water conductivity.

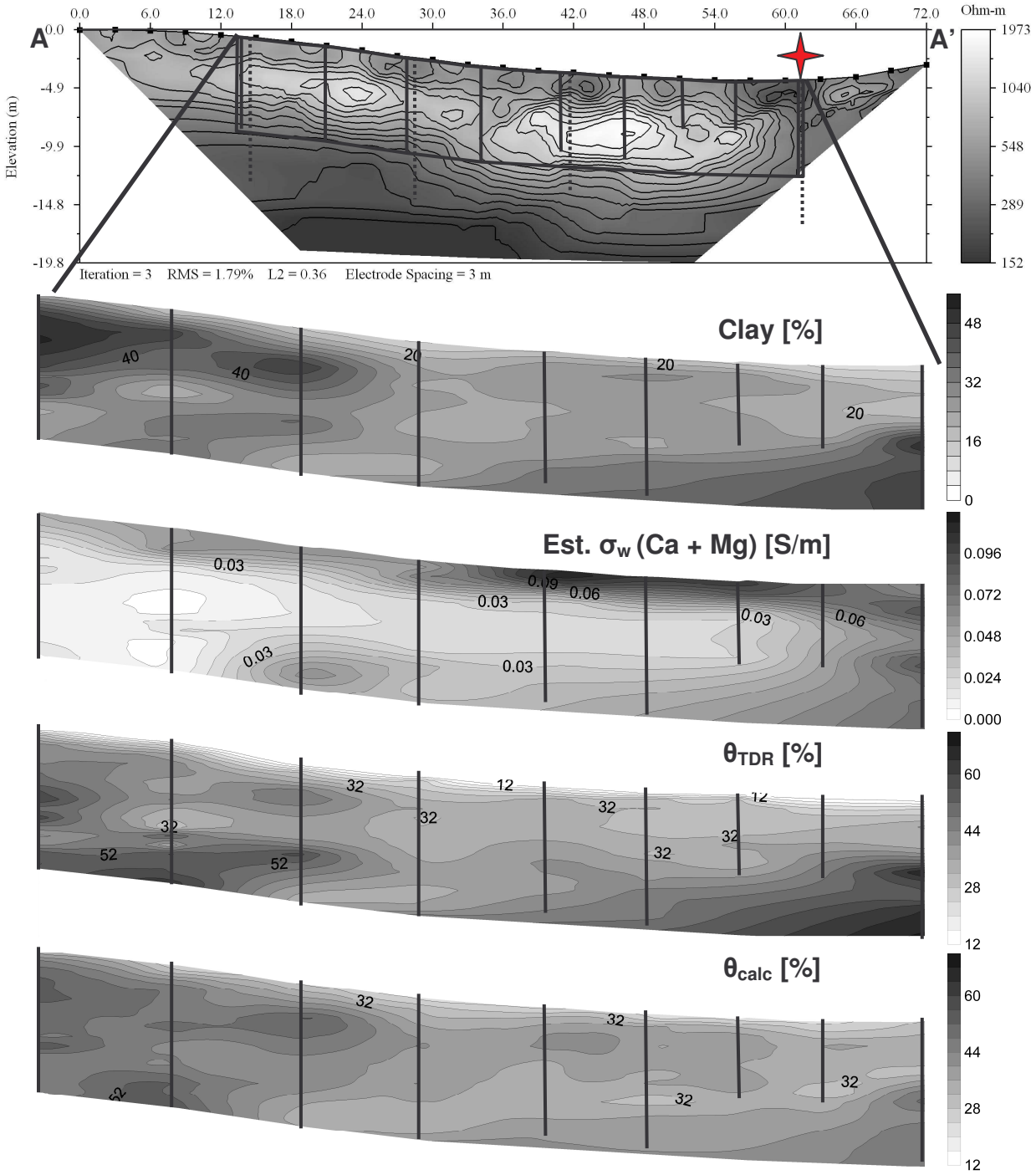

Figure 3.8 Data for sinkhole #1, profile #1
Profiles of variables interpolated between access-tubes where samples were collected from A to A' in sinkhole #1. These variables were used to produce the soil moisture profile labeled θ_{calc}. Note the similarities between this profile and the profile for θ_{TDR}. Also notice how soil moisture and ERT are related to the distribution of % clay and estimated σ_w. Note that units of [S/m] for estimated pore water conductivity are not true conductivity and are instead an estimate based on the Ca and Mg proxy.

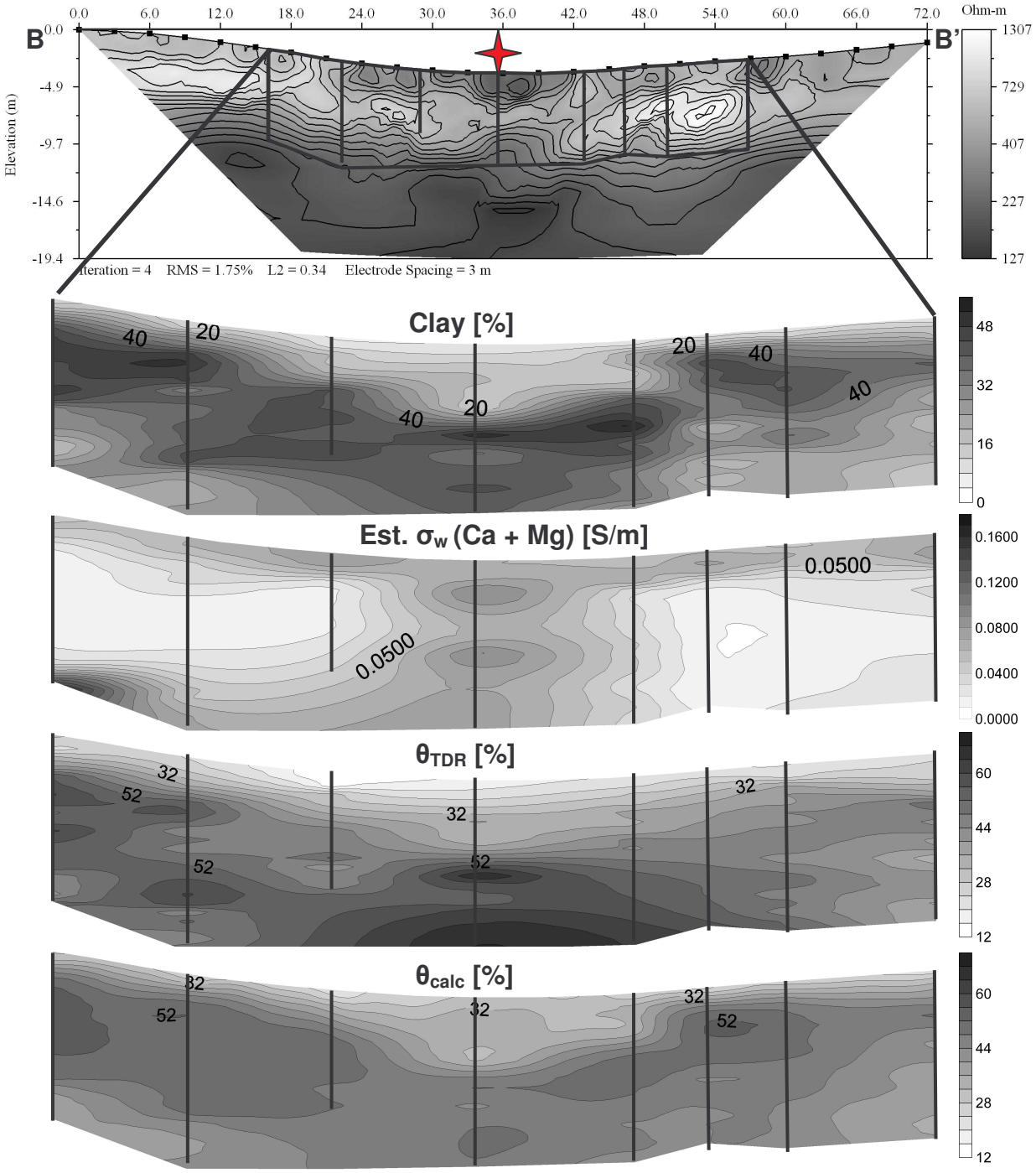

Figure 3.9 Data for sinkhole #1, profile #2

Profiles of variables interpolated between access-tubes where samples were collected from B to B' in sinkhole #1. These variables were used to produce the soil moisture profile labeled θ_{calc}. Note the similarities between this profile and the profile for θ_{TDR}. Also notice how soil moisture and ERT are related to the distribution of % clay and estimated σ_w. Note that units of [S/m] for estimated pore water conductivity are not true conductivity and are instead an estimate based on the Ca and Mg proxy.

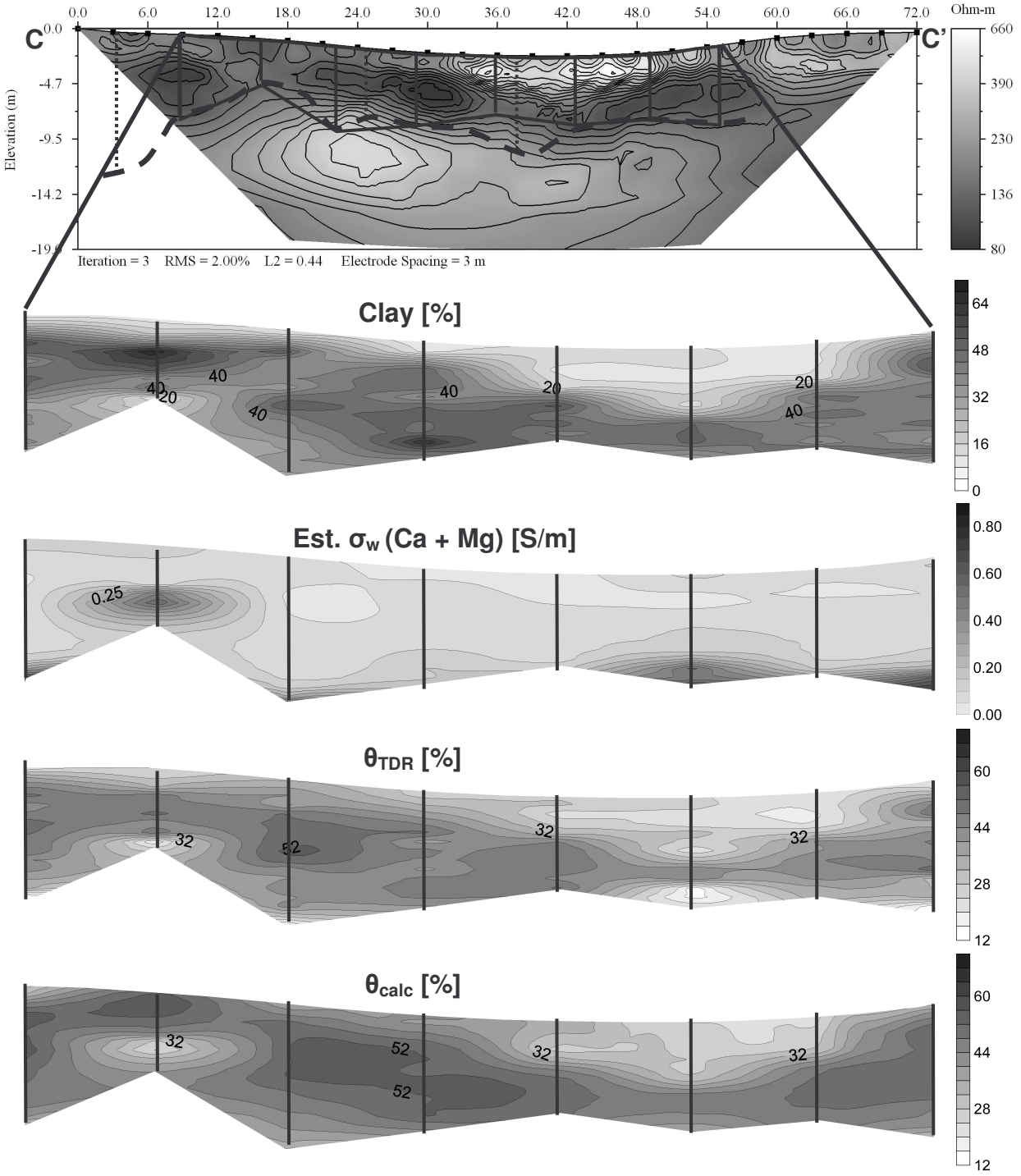

Figure 3.10 Data for sinkhole #5, profile #1
Profiles of variables interpolated between access-tubes where samples were collected from C to C' in sinkhole #5. These variables were used to produce the soil moisture profile labeled θ_{calc}. Note the similarities between this profile and the profile for θ_{TDR}. Also notice how soil moisture and ERT are related to the distribution of % clay and estimated σ_w. Note that units of [S/m] for estimated pore water conductivity are not true conductivity and are instead an estimate based on the Ca and Mg proxy.

Figure 3.10 shows these data for sinkhole #5. **Figure 3.8** is roughly perpendicular to **Figure 3.9** (see **Figure 3.1b**) and they intersect at the locations marked with a star. The general patterns in distribution of the 2-D kriged θ_{TDR} and ERT-derived θ_{calc} are very similar except for the upper 50 cm or so where θ_{calc} tends to overestimate soil moisture based on the θ_{TDR} measurements. In the near-surface, there were two important reasons for this. First, the methods we used to protect the top of our access tubes from agricultural activities resulted in the upper ~50 cm being shielded from infiltration and led to a gradual drying around the tops of the access tubes between the time of installation and the time at which these measurements were taken. The second layer of PVC (the 4 inch (10.1 cm) schedule-40 protective casing) also artificially decreased θ_{TDR}. These factors led to θ_{TDR} values which were skewed towards being drier than they actually were in the unaffected surrounding soils. Secondly, the 3 m spacing of our ERT electrode arrays resulted in lower model sensitivity to electrical properties at or just below the surface in the regions between electrodes. Additionally, the 12 inch (30.5 cm) long ERT electrodes were permanently installed 13 inches (33 cm) deep and this resulted in measurements which were skewed towards representing the damper (and more electrically conductive) soils near the bottom of the electrodes.

Also, θ_{calc} tended to produce smoother contours than are shown in the kriged θ_{TDR} data. This is primarily the result of the insensitivity of ERT models to small-scale heterogeneities (relative to the scale of ERT measurements) in soil moisture and physical properties which were clearly apparent in both θ_{TDR} measurements and in measured physical and chemical properties. **Figure 3.8, Figure 3.9,** and **Figure 3.10** allow visual comparisons between the 2-D distributions of θ_{calc} and θ_{TDR} and highlight this difference. The range of θ_{TDR} was more than twice that of θ_{calc}, which was from approximately 28 to 52 percent moisture. However, the highest and lowest values of θ_{TDR} were usually found in small regions rather that being consistently high or low over large areas. One exception is found in the lowest portions of profiles in sinkhole #1 where a region of high θ_{TDR} is not well represented by θ_{calc} (**Figure 3.9**). It is possible that the access-tube here penetrates a small-scale region of high soil moisture which is not representative of the larger-scale conditions. During augering, we observed significant heterogeneity in soil moisture at the scale of 10 cm or less. As examples, it was common to find ancient root casts or very thin layers of gravel which were acting as tiny conduits carrying water through relatively drier surrounding soils. Some of these small scale features are clearly visible in profiles of percent clay and in θ_{TDR} in **Figure 3.8, Figure 3.9,** and **Figure 3.10.**

By collecting and characterizing a large number of soil samples, we were also able to develop generalized soil profiles for each transect. In addition to characterizing soils by chemical analysis, particle size analysis and soil moisture, we also recorded detailed color information and the location of gravel and cobble-rich layers, which were not represented in the particle size analyses. In combination, these data produced an extremely complex and heterogeneous map of soils at our field site. By grossly grouping soils based on colors (which provide information about weathering history, age, and parent materials (White, 1977)) and textures, we created **Figure 3.11**. Of note is the fact that our ERT profiles (**Figure 3.5**) generally displayed patterns which could be correlated with several of the gross soil layers shown in **Figure 3.11**. As examples, the higher resistivity region near the surface in the bottom of sinkhole #5 corresponds well with an observed lens of what is essentially topsoil which eroded off the flanks and was deposited in the bottom of the sinkhole. ERT profiles in sinkhole #1 show several regions of higher resistivity values which correlate well with observed layers of very hard, dark red and high clay content soils. There are also areas where patterns in the ERT profiles appear to correlate with patterns in the distribution of percent clay, soil moisture or σ_w, though the patterns are not consistent across the entire profile. These results supported what the ERT vs. θ_{TDR} data indicated, which was that there is no simple relationship between these two parameters without first applying a model which includes the effects of certain physical and chemical parameters.

During the planning stages of this research, we assumed that the soil bedrock interface at the study site would be between 2 and 5m below the surface. This was based on verbal communications with people who had drilled to the bedrock-soil interface in nearby locations. We were surprised by the depth of soils in and around the study sinkholes - especially in sinkhole #1. One reason we initially chose ERT to image the subsurface was the fact that others have successfully imaged the soil-bedrock interface using ERT (Zhou et al., 2000). In our case, ERT did not clearly detect the interface in sinkhole #5 (**Figure 3.5** and **Figure 3.11)**. In fact, without ground-truthing by augering, we would not have determined that the bedrock-soil interface was within the depth of resolution for our ERT measurements. Many of the resistivity contrasts which were initially identified as possible soil-bedrock interfaces (in ERT profiles obtained prior to augering) were actually contrasts in soil texture, soil moisture and other physical properties. We believe there are two important reasons why we did not detect the soil-bedrock interface with ERT in sinkhole #5: 1) the Elbrook Formation is locally highly fractured

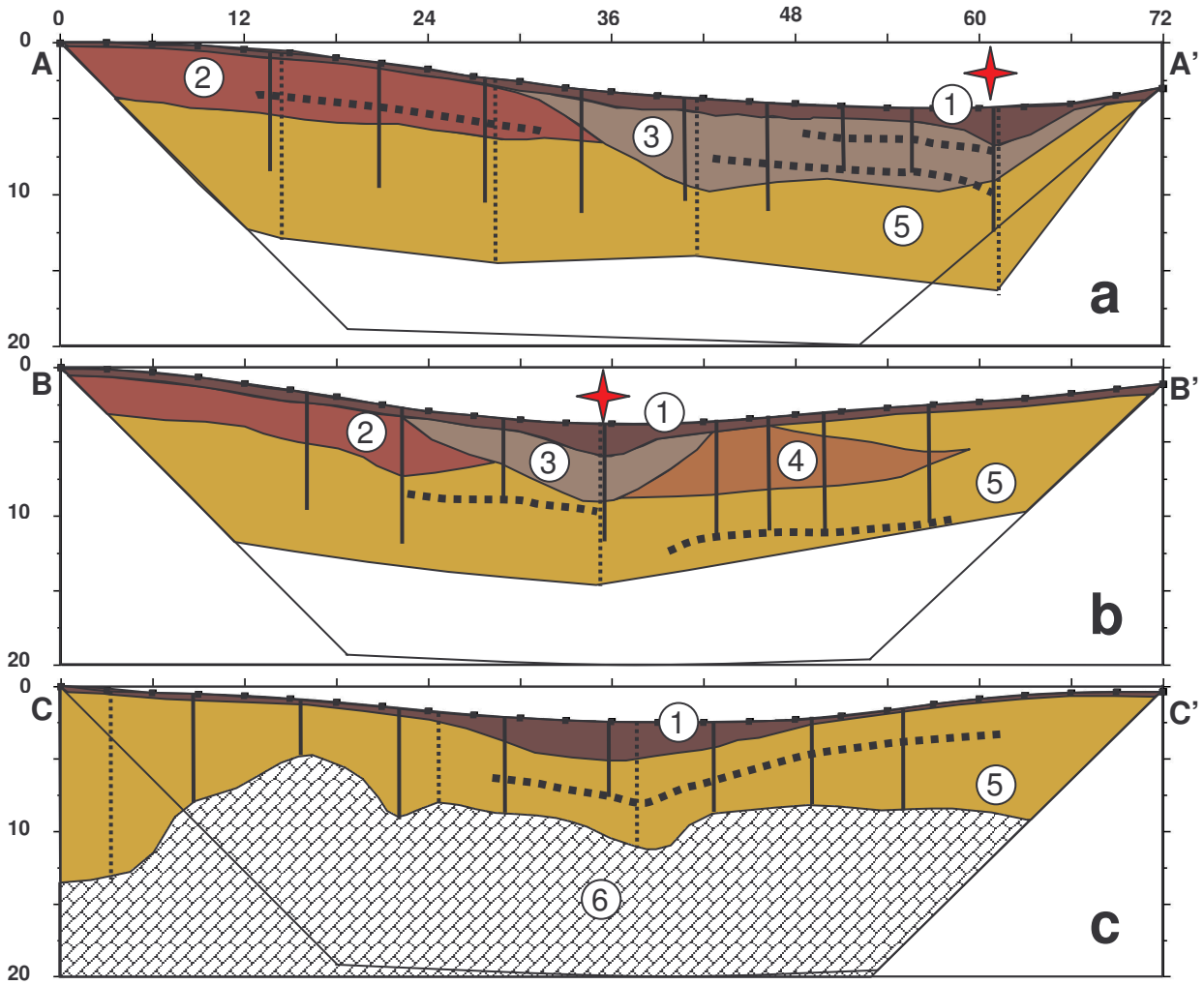

Figure 3.11 Generalized profiles of gross soil texture and color
Interpretations of gross soil texture, color, and horizonation for each transect in sinkhole #1 (a and b) and sinkhole #5 (c). Circled numbered zones: 1) represents dark yellow brown loam, clay loam, sandy loam, and silt loam (A horizons), 2) is hard and generally drier dark red clay loam, silty clay loam and silty clay (Bt horizons), 3) is light grey to yellow grey sandy clay loam, sandy loam and loam (Btg and Bg horizons), 4) is a reddish orange clay loam, silty clay loam and silty clay (Bt horizons), 5) is a brownish yellow to yellow silty clay, silty clay loam and clay loam (Bt and C horizons), and 6) is carbonate bedrock. Bold dashed lines represent interpreted cobble and gravel layers. The star in a) and b) indicates the location at which transects a) and b) intersect. Profile endpoints A, A', B, B', C and C' represent end points on transects shown in **Figure 3.1**. We emphasize that these interpretations are only based on gross soil characteristics and do not represent the true heterogeneity of the system in terms of textures, cobble and gravel content, or color. Soils in these profiles fall into all USDA soil texture classes except for sand, and are widely distributed across the USDA textural triangle with no clear patterns. Solid vertical lines represent access-tubes and dashed lines represent monitoring wells. Interpretations extend beyond the outline of our ERT profiles where we have information from monitoring wells. All units are in [m].

and weathered because of our field site's proximity to the edge of the Pulaski thrust sheet (Commonwealth of Virginia, 2003), and 2) the uppermost region of weathered bedrock has both high clay and moisture content. It is also worth pointing out that the highest resistivity values in sinkhole #5 are less than 700 Ohm-m and were actually measured in the well-drained silty soils in the bottom of this sinkhole rather than in the underlying bedrock. These are all important factors to consider when using ERT in similar geologic settings and reinforce the fact that ERT is best used in conjunction with physical data to validate interpretations.

To obtain the most accurate soil moisture models, it is important that accurate ERT measurements be collected. Obtaining ERT profiles with minimized measurement error can be difficult and may require methods for data collection in the field which are more exacting than are required for an ERT profile designed to grossly characterize features in the subsurface. Perhaps the most important factor in the field is ensuring good electrical contact between ERT electrodes and the soils. Our method of installing permanent carbon electrodes minimized measurement error and produced higher quality data than we were able to obtain using traditional metal electrodes inserted at the surface. Though it is certainly more time consuming than using metal electrodes at the surface, we recommend this method if long term studies of soil moisture are planned.

CONCLUSIONS

We have developed a new method for determining field-scale 2-D soil moisture distribution using 2-D electrical resistivity tomography (ERT) measurements with 1-D soil moisture and physico-chemical properties of the soil. Our methods are easy to apply to nearly any field site where a quantitative assessment of 2-D soil moisture distribution is desired. We have shown that these methods will produce useful results in heterogeneous settings and that meter-scale soil moisture variations can easily be detected and modeled. Our model results do not resolve small scale heterogeneities in soil moisture measured with TDR, but instead represent a smoother model which reflects the inability of ERT measurements to measure small-volume features at this scale. For example, small regions of high or low moisture as measured in a 1-D TDR moisture profile, and which span at most 30 cm, are unlikely to be resolved using an ERT array with 3m electrode spacing. Our field site contains extremely heterogeneous soil profiles because the soils are derived from weathered ancient fluvial terrace deposits. In more homogeneous

systems, lower resolution sampling of physical/chemical measurements may be required to achieve the same level of accuracy in moisture prediction.

A specific setting where our methods might be particularly useful in determining soil moisture distribution is in thick soils - especially in clay-rich soils where tools such as GPR can not be used to image subsurface features because of signal attenuation problems. Another very important application of these techniques would be to quantitatively assess volumetric moisture changes over time by collecting time-series data. Results of this type of study can be used to address important hydrogeologic questions such as how much, where, and when do infiltration and recharge occur in different unsaturated hydrogeologic settings? With the current capabilities of ERT equipment and inversion software to both collect and model 3-D ERT data, these same methods can also be applied to understanding 3-D soil moisture distribution both spatially and temporally.

Showing that extractable cations can be used as a proxy for pore water conductivity in a numerically optimized form of Archie's Law was an especially important result of this research, particularly for soils with very low soluble salts. By using extractable cations, we eliminated the difficult and time consuming task of measuring pore water conductivity and instead used data which are easy to obtain by a standard soil analysis. Depending on the soil characteristics at other sites, different extractable cations may need to be used to obtain the best results.

ACKNOWLEDGEMENTS

We acknowledge funding for this research from: US Department of Education GAANN Fellowship, Virginia Water Resources Research Center, Cave Conservancy Foundation, Cave Research Foundation, National Speleological Society, Geological Society of America, West Virginia Association for Cave Studies, and the Virginia Tech Graduate Research Development Program. We thank Ankan Basu, Mike Beck, Lee Daniels, Beth Diesel, Bruce Dunlavy, Frank Evans, Brad Foltz, Marty Griffith, Mary Harvey, Ashley Hogan, Danielle Huminicki, Stuart Hyde, Rachel Lauer, Steve Nagle, Jeanette Montrey, Wil Orndorff, Zenah Orndorff, Dave Rugh, Cori and Zachary Schwartz, Jim Spotila, Brett Viar, Dongbo Wang, and Brad White for their assistance both in the field and in the lab.

REFERENCES

Advanced Geosciences, I. 2005. EarthImager 2D.

Archie, G.E. 2003. Electrical resistivity log as an aid in determining some reservoir characteristics. Society of Petroleum Engineers reprint series: 9-17.

Auerswald, K., S. Simon, and H. Stanjek. 2001. Influence of soil properties on electrical conductivity under humid regimes. Soil Science 166:382-390.

Barker, R., and J. Moore. 1998. The application of time-lapse electrical tomography in groundwater studies. The Leading Edge October:1454-1458.

Commonwealth of Virginia. 2003. Digital Representation of the 1993 Geologic Map of Virginia, Publication 174. Department of Mines, Minerals and Energy, Division of Mineral Resources.

Daily, W., and A. Ramirez. 2000. 200 East Vadose Test Site, Hanford Washington, Electrical Resistivity Tomography. Lawrence Livermore National Laboratory, Livermore, CA.

Dane, J.H., Topp, G.C., (ed.) 2002. Methods of soil analysis. Part 4: physical methods, pp. 1-1692. Soil Science Society of America, Madison, Wisconsin.

Harris, W.G., S.S. Iyengar, L.W. Zelazny, J.C. Parker, D.A. Lietzke, and W.J. Edmonds. 1980. Mineralogy of a chronosequence formed in New River alluvium. Soil Science Society of America Journal 44:862-868.

Hauck, C., and A. Scheuermann. 2005. Comparing Time Domain Reflectometry and Electrical Resistivity Tomography Measurements for Estimating Soil Water Distribution. 11th European Meeting of Environmental and Engineering Geophysics (Near Surface 2005).

Jacobsen, O.H., and P. Schjonning. 1993. A laboratory calibration of time domain reflectometry for soil water measurement including effects of bulk density and texture. Journal of Hydrology:147-157.

Kalinski, R.J., and W.E. Kelly. 1993. Estimating water content of soils from electrical resistivity. Geotechnical Testing Journal 16:323-329.

Kalinski, R.J., W.E. Kelly, I. Bogardi, and G. Pesti. 1993. Electrical resistivity measurements to estimate travel times through unsaturated ground water protective layers. Journal of Applied Geophysics 30:161-173.

Lambot, S., J. Rhebergen, I.v.d. Bosch, E.C. Slob, and M. Vanclooster. 2004. Measuring the soil water content profile of a sandy soil with an off-ground monostatic ground penetrating radar. Vadose Zone Journal 3:1063-1071.

Maulem, Y., and S.P. Friedman. 1991. Theoretical prediction of electrical conductivity in saturated and unsaturated soil. Water Resources Research 27:2771-2777.

Michot, D., Y. Benderitter, A. Dorigney, B. Nicoullaud, D. King, and A. Tabbagh. 2003. Spatial and temporal monitoring of soil water content with an irrigated corn crop cover using surface electrical resistivity tomography. Water Resources Research 39:1138.

Mullins, G.L., Heckendorn, S. E. 2005. Draft Copy of Laboratory Procedures - Publication 452-881. Virginia Tech Soil Testing Laboratory, Blacksburg.

Poeter, E.P., M.C. Hill, E.R. Banta, S. Mehl, and S. Christensen. 2005. UCODE_2005 and Six Other Computer Codes for Universal Sensitivity, Calibration, and Uncertainty Evaluation: U. S. Geological Survey Techniques and Methods 6-A11.

Rhoades, J.D., N.A. Manteghi, P.J. Shouse, and W.J. Alves. 1989. Estimating soil salinity from saturated soil-paste electrical conductivity. Soil Science Society of America Journal 53:428-433.

Schwartz, B.F., M.E. Schreber, P.S. Pooler, and J.D. Rimstidt. *In review*. New methods for obtaining accurate access-tube TDR moisture values: a tool for understanding vadose

hydrology in deep and heterogeneous soil profiles. *In review at:* Soil Science Society of America Journal.

Shah, P.H., and D.N. Singh. 2005. Generalized Archie's Law for Estimation of Soil Electrical Conductivity. Journal of ASTM International 2:1-20.

Shuyun, L., and T.-C.J. Yeh. 2004. An integrative approach for monitoring water movement in the vadose zone. Vadose Zone Journal 3:681-692.

Titov, K., A. Kemna, A. Tarasov, and H. Vereeken. 2004. Induced polarization of unsaturated sands determined through time domain measurements. Vadose Zone Journal 3:1160-1168.

USDA-NRCS. 2006. Web Soil Survey [Online] http://websoilsurvey.nrcs.usda.gov/app/WebSoilSurvey.aspx (verified September 4, 2006).

White, W.B. 1977. Characterization of karst soils by near infrared spectroscopy. The National Speleological Society Bulletin 39:27-31.

Yao, T., P.J. Wierenga, A.R. Graham, and S.P. Neuman. 2004. Neutron Probe calibration in a vertically stratified vadose zone. Vadose Zone Journal 3:1400-1406.

Zhou, Q.Y., J. Shimada, and A. Sato. 2001. Three-dimensional spatial and temporal monitoring of soil water content using electrical resistivity tomography. Water Resources Research 37:273-285.

Zhou, W., B.F. Beck, and J.B. Stephenson. 2000. Reliability of dipole-dipole electrical resistivity tomography for defining depth to bedrock in covered karst terranes. Environmental Geology 39:760-766.